Linking leaf hydraulics with anatomy in *Populus* genotypes

by

Caroline Alexandra Brocious

A thesis submitted in partial fulfillment of the requirements for the degree of

Master of Science
in
Forest Biology and Management

Department of Renewable Resources
University of Alberta

Abstract

Global increases in carbon dioxide have refocused attention on trees as a mechanism for carbon storage. Leaves are vital to this process, serving as both the site of carbon gain and water loss in trees. As transpiration and photosynthesis are inherently linked in leaves, water movement through trees effectively controls overall carbon uptake and biomass production.

Leaf hydraulic movement is limited in turn by hydraulic resistance in the xylem and leaf lamina. Consequently, this study focused on leaf anatomy to distinguish hydraulic differences across genetically similar *Populus* genotypes. Previous work has focused on leaf hydraulic conductance across species, yet few have isolated anatomical influences on leaf conductance within a genus.

In a greenhouse study, six *Populus* genotypes were grown under standardized conditions and measured for leaf hydraulic and stomatal conductance. Anatomical areas of resistance in leaves were preserved and measured using light microscopy. Petiole hydraulic structure emerged as a strong correlate of hydraulic performance, suggesting that xylem area in the petiole supports leaf area and conductance. Overall, my research suggests that scaling in hydraulic anatomy influences performance in *Populus* leaves, and that petiole hydraulic measurements are an important component to include in future leaf hydraulic measurements.

Preface

This research was funded by an NSERC Strategic grant awarded to Drs Uwe G. Hacke, Malcom Campbell, and Barb Thomas. All data collection, measurement and analysis were performed by me, with the assistance from Dr. Uwe G. Hacke.

A version of this thesis will be submitted as Brocious, C. A. and Hacke U. G. 2015. "Stomatal conductance scales with petiole hydraulic conductance in hybrid poplar clones" in *Functional Plant Biology*. U. H. and I equally shared the responsibility for conceiving and designing the study. I performed the experiments; U.H. assisted with some of the measurements, and I wrote the main body of the manuscript. U. H. contributed to manuscript edits.

Acknowledgments

I would like to thank the many people who helped me reach this point: Firstly my supervisor, Dr. Uwe Hacke, for being such a wonderful mentor and guide. It has been such an honor to work for you – I could not have made it without your support and kindness.

Additionally, I would like to thank my supervisory committee: Dr. Janusz Zwiazek and Dr. Andreas Hamann. Janusz, I learned so much from you in my first year – I am so glad I took Tree Physiology! Andreas, you have supported me from afar throughout my degree – thank you so much for your guidance and wisdom.

I would also like to thank my lab mates: Rachel Hillabrand, Ryan Stanfield, Jaime Azcona, and especially Joan Laur and Stefan Schreiber. You listened patiently through my endless questions, and never failed to help me out when I needed it. Barb Thomas and Dave Kamelchuk – thank you for teaching me so much about hybrid poplars. Thank you for working with Al-Pac to provide me with trees. I hope our plantation at the Devonian Garden flourishes one day!

I would also like to thank my parents, who continually supported and encouraged me through this degree. Mom and Dad, you never stopped cheering me to greatness ("Cay-la! Cay-la!"). I promise to repay the favor and take care of you both in your old age! Dave, you were my strong, loving foundation through this process – I cannot wait for our adventures together. And to my dog, Ulfur – you loved me whether I had a degree or not. Thank you all for being part of this chapter in my life.

Lastly, I would like to thank my funding sources – NSERC, the Department of Renewable Resources, and FGSR Travel Award – for making my research possible.

Table of Contents

List of Tables and Equations

List of Figures

1 Introduction

1.1 Overview

"Leaves mediate the fluxes of resources and energy in all terrestrial ecosystems. They are a fundamental energetic unit of biology." – Blonder et al. 2011

Over the past century, global concentrations of atmospheric carbon dioxide (CO_2) have increased at an unprecedented rate. Forests, which cover ~30% of the globe, are increasingly vulnerable to escalating temperature and drought events and have experienced significant die-back in recent years (Allen et al. 2010, Michaelian et al. 2011). Trees have the potential to combat increasing CO_2 levels by acting as a carbon storage system, yet are limited in carbon uptake by water availability.

Currently, many forests and commercial plantations in North America are dominated by *Populus* pure species and hybrids. Hybrid poplars, or crosses between two trees from the *Populus* genus, are valued worldwide for high rates of carbon uptake, also known as productivity. Producing up to 30 Mg ha^{-1} yr^{-1} of woody biomass (Bradshaw et al. 2000), poplars are a valuable resource for carbon storage. Aspen, *Populus tremuloides* Michx., is the most wide-spread tree in North America (Schreiber et al. 2011), and thus represents a significant amount of carbon biomass. However, aspen is currently experiencing severe drought-induced mortality from increasing temperatures and water scarcity (Allen et al. 2010, Michaelian et al. 2011). By better-understanding how trees move water under ideal conditions, we can deepen our knowledge of how trees and forests will respond to drought.

Most of our knowledge about water movement in poplars comes from studies at the tree, stem and branch level (Barigah et al. 1994, Arango-Velez et al. 2011, Schreiber 2011, 2013, Hacke 2015). However, leaves may be the first organs to react to decreased water availability. Under drought stress, trees react by first closing their stomata which reduces water loss from transpiration. Unfortunately, this in turn restricts gas exchange and subsequent photosynthesis. Therefore, understanding the trade-offs leaves make at a stomatal level will help us understand ultimate carbon uptake.

Many questions still remain about water movement through leaves, which account for approximately 30% of the whole-plant resistance to water flow (Sack and Holbrook 2006, Brodribb 2007). The present research addresses this gap and seeks to understand if hydraulic movement is influenced by leaf anatomy of *Populus* genotypes. Great diversity exists in leaf morphology and performance among poplar species, making the *Populus* genus a perfect study system. This research seeks to provide insight on anatomical components of hydraulic conductance to ultimately deepen our understanding on factors limiting CO_2 uptake and water movement.

1.2 Leaves

1.2.1 Leaf structure

Leaves are incredibly diverse in shape and size (Sack et al. 2012), yet are commonly ascribed one function: photosynthesis. This process ($6\ CO_2 + 12\ H_2O \rightarrow C_6H_{12}O_6 + 6\ O_2 + 6\ H_20$) is responsible for global carbon uptake and oxygen production, and takes place in leaf mesophyll

(Pallardy 2010). Water is supplied to the mesophyll through leaf veins, which taper in size from the midvein to secondary and smaller (Fig. 1.1). A branch supports the leaf by means of a petiole, which is largely composed of the vascular bundle (Fig. A1).

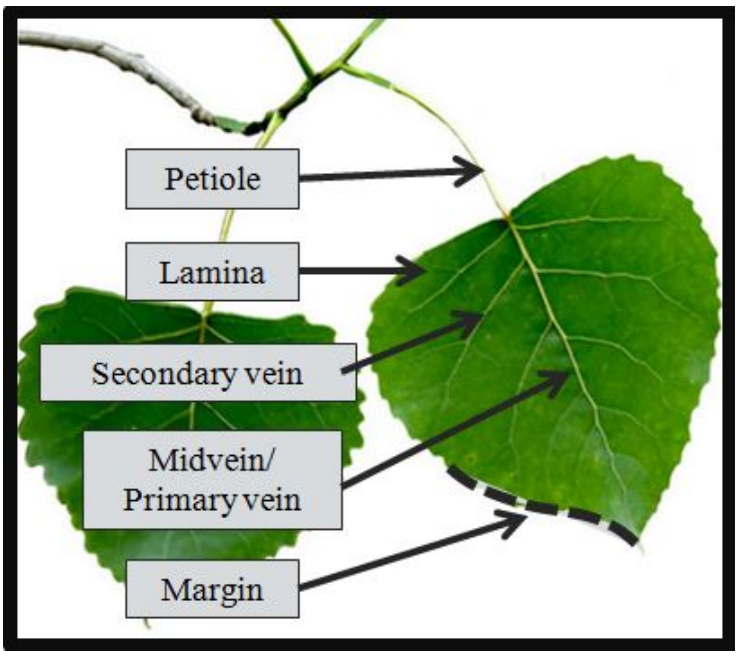

Figure 1.1: Labeled diagram of external leaf anatomy. The leaf blade or lamina is attached to the stem by the petiole, which connects vascular tissue from the stem to the primary vein. Secondary veins distribute water across the lamina, sometimes all the way to the margin.

However, photosynthesis in the leaf involves a tradeoff between carbon uptake and water loss. While photosynthesis and water transport are separate processes, they are inherently linked through transpiration (Brodribb 2009). As CO_2 is exchanged through open stomata on the underside of the leaf, water transpires out from the moist mesophyll to the dry atmosphere (Zwieniecki 2002, Brodribb 2009, Sack and Holbrook 2006). As a result, great pressure is

placed on leaf hydraulic architecture to efficiently supply the mesophyll with water (Zwieniecki 2002), which is in turn influenced by the leaf's internal hydraulic anatomy (Sack et al. 2015).

Inside the leaf, a complex system is responsible for water movement: xylem venation and the extra-xylem pathways (Fig. 1.2 and 1.3, Sack et al. 2012, Buckley 2015, Scoffoni 2015). Xylem venation can be analyzed from two different perspectives, either from a surface-view (the venation architecture), or as a cross-section. The extra-xylem pathway potentially includes xylem parenchyma cells, the bundle sheath, the bundle sheath extensions, and the mesophyll (Shatil-Cohen 2012, Buckley 2015, Scoffoni 2015, Sack et al. 2015). This last traverse of water from the vein ends to the epidermis has been suggested to limit overall hydraulic efficiency and photosynthesis (Brodribb et al. 2007), which could have profound effects on growth.

Many questions remain unanswered as to the final resistance to hydraulic flow, yet a recent study sought to model extra-xylem hydraulic conductance in the mesophyll (Buckley 2015). Overall, Buckley (2015) determined that the flow path strongly depended on leaf anatomy, but that the bulk of liquid water flow occurs through apoplastic movement (Scoffoni 2015). As such, my research proposes to take into account aspects of apoplastic flow through poplar leaves, including minor vein area, area of the bundle sheath extensions, distance to the lower epidermis, and overall lamina thickness. In summation, many internal and external factors may influence photosynthesis and leaf hydraulics (Sack and Holbrook 2006), but this study focuses on potentially limiting structural parameters in the petiole, leaf veins, and internal anatomy.

1.2.2 Leaf hydraulic conductance as an estimate of performance

Research in leaf hydraulics over the past 20 years has focused on one parameter characterizing hydraulic performance: K_{leaf}. K_{leaf}, the abbreviation for leaf hydraulic conductance, is a measure of how efficiently water moves through the leaf, calculated by flow over driving force (see Eqn. (1) in 3.3.1; Sack and Holbrook 2006). As it summarizes a "complex micro-hydrological system" within leaves (Sack et al. 2015), K_{leaf} encompasses water flow both within and outside the xylem for the whole leaf (Sack and Holbrook 2006).

Previous studies have linked K_{leaf} to photosynthesis, stomatal conductance, carbon assimilation, vein length per area (VLA), and numerous other traits corresponding to anatomy and physiology (Nardini et al. 2014, Sack et al. 2015). However, most of these studies have concentrated on multiple species in an attempt to derive global patterns of K_{leaf} (Sack and Holbrook 2006, Brodribb et al. 2007). In contrast, remarkably few studies have focused on K_{leaf} and anatomy within a species (specifically Nardini et al. 2014, Xiong et al. 2014, Caringella et al. 2015). My research endeavors to fill the existing gap in K_{leaf} and anatomical influences by measuring six genotypes within the *Populus* genus.

1.3 Examining the hydraulic pathway: leaf veins and vessels

1.3.1 Evolution of the leaf and leaf veins

Around 450 million years ago, plants moved from the hydric environments typical of bryophytes to the dry, exposed, terrestrial environment (Boyce 2008, Boyce et al. 2009, Brodribb 2009). To

survive in a new environment, plants developed two morphological changes: a cuticle and a vascular system (Lucas et al. 2013). The cuticle, a moderately waterproof, waxy layer of cutin on the epidermis, prevented the sensitive plant tissue from moisture loss and solar radiation (Pallardy 2010, Sperry 2003). However, the evolution of the vascular system had the greatest impact on plant survival (Lucas et al. 2013) and resulted in the diversity we see in angiosperms today.

The vascular system developed through specialization of primitive water conducting cells, likely resulting from selection pressure and a higher demand for water than CO_2 during the Carboniferous period (Sperry 2003, Lucas et al. 2013). Over time, vascular plants developed a "skeleton" of dead cell walls to conduct water that greatly increased hydraulic conductivity (Sperry 2003). This was crucial to megaphyte development, as plants were no longer restricted in size. Previously, plants could only efficiently hydrate a few layers of cells due to the physically slow process of symplastic diffusion (Lucas et al. 2013). Additionally, the lignified vascular system also provided mechanical support (Sperry 2003). This allowed plants to grow taller and deeper underground to reach water and nutrients (Beerling 2005, Lucas et al. 2013).

Now upright and sufficiently hydrated, plants needed to develop primitive leaves to maximize sunlight absorption and photosynthesis (Lucas et al. 2013). Early fossil records show stunted, aerial stems bearing miniature leaves (termed microphylls), evidence of a trend that presided over the Paleozoic (Beerling et al. 2001, Beerling 2005). The high levels of atmospheric CO_2 and solar radiation meant that larger leaves were a disadvantage to the plant, as they would overheat and render photosynthesis inefficient (Beerling et al. 2001, 2005). It was not until CO_2

levels drastically declined in the late Paleozoic that megaphylls became beneficial to the plant (Beerling 2005).

For angiosperms, most of this benefit derives from the netted, reticulate venation structure of their leaves. Fossil evidence shows that reticulate venation evolved four distinct times over the past millennia (Zwieniecki et al. 2002, Boyce 2008), indicating that some hydraulic benefit must be supported by increased venation. While ferns and seed plants also had leaf veins, angiosperms had uniquely high density of veins (Boyce 2008, Boyce et al. 2009, Brodribb and Feild 2010). Indeed, current measurements attest that angiosperms have 8-20 mm of vein length per mm^2 of lamina (Boyce 2008, Sack et al. 2012). Leaf veins supported both xylem and phloem movement, and therefore carbon assimilation and transpiration rates. Clearly, high vein density offered a functional advantage to angiosperms, indicating an optimal strategy between carbon uptake and water loss (Boyce et al. 2009, Brodribb 2009).

1.3.2 Vein formation

However, the fossil record is bereft of information on how leaf veins form. It is only through modern technology that we are able to understand tissue differentiation in the meristem that produces angiosperm leaf. In leaves, veins have two main objectives: transport through the vascular bundle and structural support of the lamina (Zwieniecki et al. 2002, Blonder et al. 2011). The main function of the vascular bundle is transport: water to the leaves, and photosynthate to the stem and roots. As hydraulic transport is half of this function, my research will center on this component in leaf veins. Veins taper in importance and size throughout the leaf (Brodribb et al. 2009). Larger veins distribute water across the lamina, but the smaller veins hydrate the mesophyll (Sack and Holbrook 2006) and collect many of the sugars produced by

photosynthesis. Additionally, minor veins account for the bulk of vein length per area in the leaf (Sack et al. 2009, Sack and Scoffoni 2013). For this reason, leaf veins are usually ordered by size and classified in terms of leaf venation architecture (Fig. 1.2; Ellis et al. 2009).

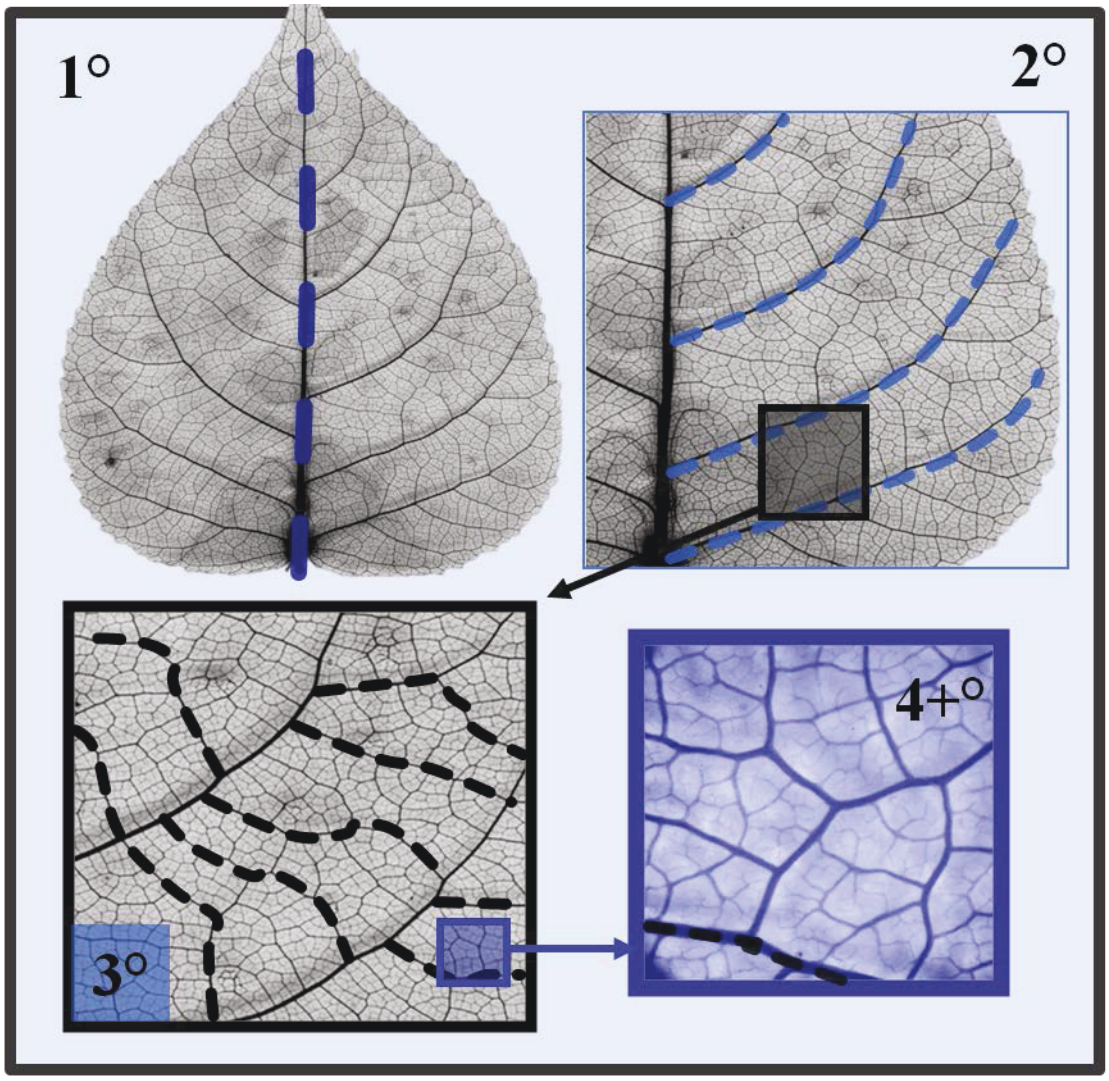

Figure 1.2: Vein orders in *Populus* sp. leaves. Veins decrease in diameter from primary (1°) down to quaternary and higher (4+°). All veins in the lower right blue box are 4+ veins (apart from the dashed black line, which is 3°). Poplar leaves have brochidodromous secondary veins, meaning loops form at the margin (classified from Ellis et al. 2009).

For most angiosperm leaves, the hydraulic architecture is composed of primary, secondary, tertiary, and higher order veins (Fig. 1.2; Sack and Scoffoni 2013), which develop during two distinct phases of morphogenesis (Scarpella et al. 2004, 2006, 2010, Sack et al. 2012). In the leaf primordia, different localizations of the hormone auxin turn procambial cells into vascular strands, which over time develop into vascular tissue (Scarpella et al. 2004, 2006, 2010). The first stage of this development is called primary morphogenesis, and is characterized by rapid cell division which creates the primary and secondary veins (Scarpella et al. 2010, Sack et al. 2012). Stomatal cells are also initiated during this phase (Cairns-Murphy et al. 2014). Next, secondary morphogenesis occurs, which creates higher order veins (tertiary and higher) as the leaf expands (Scarpella et al. 2010, Cairns-Murphy et al. 2014). The separation between these two processes fundamentally impacts vein patterns in expanding leaves and hydraulic relations (Sack et al. 2012).

1.3.3 Vessels in the xylem

In angiosperm leaves, the xylem is composed mainly of vessel elements, with some tracheids in the minor veins (Zwieniecki et al. 2002). My study chose to focus on xylem because it may account for almost 60% of total resistance to water flow (Sperry et al. 2006) and because it remains difficult to quantify the extra-xylem resistance in leaves. Hydraulic flow through structures like petioles or leaf veins is difficult to measure directly, but can be estimated by employing the Hagen-Poiseuille equation (Hagen 1939, Poiseuille 1940; Schultz and Matthews 1993, Tyree and Ewers 1991, Tyree and Zimmerman 2002). It is important to note that the Hagen-Poiseuille equation was created to describe flow in perfect cylindrical pipes, which is

quite different from the lumens of vessel elements and tracheids found in *Populus* xylem (see Eqn. (2) and (3) in 2.4.4).

Flow through vessels is constrained by perforation plates (Tyree and Ewers 1991) and pit membranes (Sperry and Hacke 2004, Wheeler et al. 2005). Pit membranes exert the largest resistance to water flow, because they must also prevent air-seeding and xylem cavitation (Sperry and Hacke 2004, Hacke et al. 2006). This high hydraulic resistance in the xylem means that calculated flow will always be an overestimate, on average two or more times larger than measured flow (Schulz and Matthews 1993, Tyree and Ewers 1991). However, the overestimate will be more or less constant for all xylem vessels, meaning that the rankings of *Populus* genotypes used in this study will remain constant.

Xylem vessels usually taper from roots to stems to leaves (Tyree and Ewers 1991, Hacke and Sauter 1996), meaning that vessels in the leaf will have a relatively smaller diameter than the stems. Smaller vessels in the xylem usually correlate with cavitation resistance, or the ability to resist embolism formation, from drought or freezing stress (Tyree and Zimmerman 2002, Schreiber et al. 2013). Many studies have focused on leaf vulnerability to cavitation in the past 15 years, especially relating to changes in water status, seasonal variation, and irradiance (Voicu et al. 2008, Voicu and Zwiazek 2011, Scoffoni et al. 2011, Nardini et al. 2014). One recent study found that *P. trichocarpa* leaves were highly sensitive to drought, which relates to vessel diameter and stomatal regulation (Laur and Hacke 2014a). However, the current study focuses only on leaf hydraulics at maximum conductance and hydration.

1.3.4 Hydraulic movement through the extra-xylary pathway

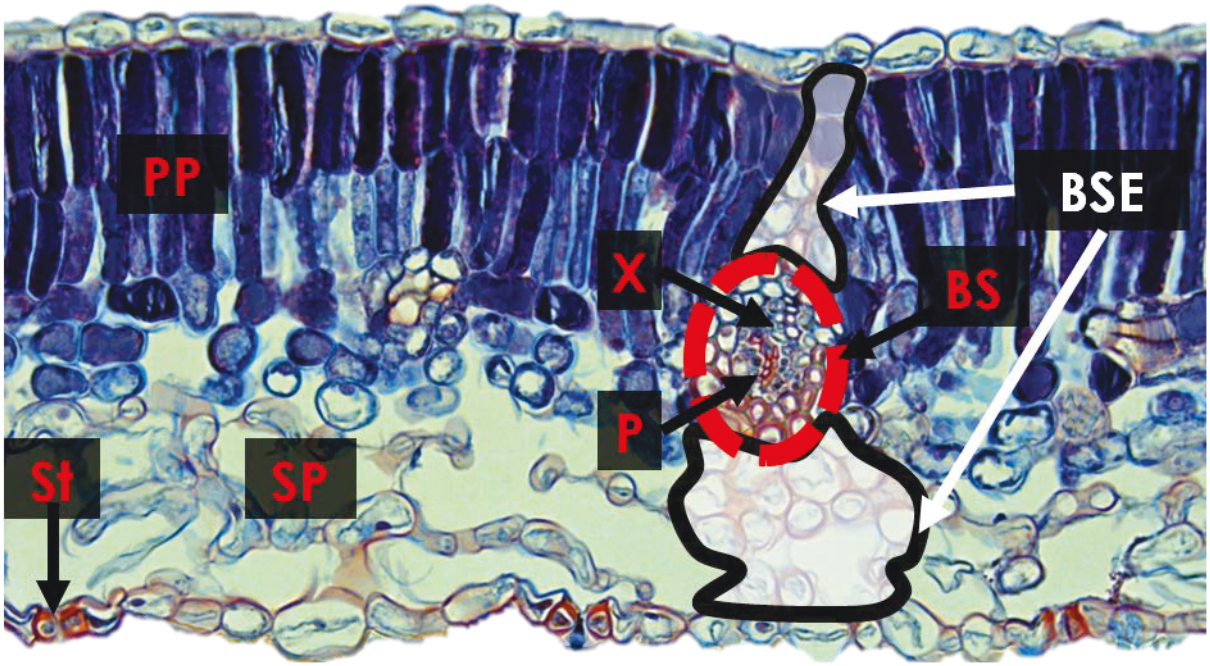

Figure 1.3 Lamina cross-section detailing the internal anatomy. The palisade parenchyma (PP) is oriented at the top of the leaf, above the spongy mesophyll (SP) and stomata (St). The xylem (X) and phloem (P) are positioned inside the bundle sheath (BS), which encircles the minor vein. Bundle sheath extensions (BSEs) extend to the adaxial and abaxial surface.

Leaf anatomy is increasingly recognized as a key determinant of hydraulic and photosynthetic performance in leaves (Sack and Holbrook 2006, Brodribb et al. 2007, Buckley 2015). Current research has focused on the extra-xylem pathway as the limiting factor to leaf hydraulic conductivity (Brodribb et al. 2007, Sack et al. 2015). In particular, aspects such as bundle sheath anatomy, minor vein density, and mesophyll thickness are thought to play a large role in overall hydraulic conductance and photosynthesis (Aasama et al. 2001, Sack and Frole 2006, Brodribb et al. 2007). This hydraulic resistance occurs through three components of the extra-xylem

pathway: the bundle sheath, bundle sheath extensions, and distance from the xylem to the evaporating surface (Figure 1.3).

For water to leave the xylem in minor veins, it must first cross the bundle sheath - a layer of parenchyma cells that encircle the vascular bundle (Shatil-Cohen et al. 2011, Pallardy 2010). The bundle sheath has recently been described as a bottleneck to leaf hydraulic conductance (Ache et al. 2010, Shatil-Cohen et al. 2011), and is now believed to be a control point for all leaf hydraulic function (Sack et al. 2015).

Bundle sheath cells function by isolating the vascular bundle from the surrounding mesophyll, preventing apoplastic water flow. The bundle sheath is believed to regulate symplastic water movement, likely resulting from up- or down-regulating aquaporin activity (Heinen et al. 2009, Shatil-Cohen et al. 2011). Aquaporins are integral membrane proteins that regulate water movement (Martre et al. 2002, Shatil-Cohen et al. 2011, Laur and Hacke 2014). Laur and Hacke (2014b) found that aquaporins assisted foliar hydration across the endodermis-like bundle sheath of needles. Pertinent to this study, the aquaporin family in poplar leaves has been characterized and shown to aid in hydraulic recovery of leaf hydraulic conductance (Almeida-Rodriguez et al. 2010, Laur and Hacke 2014b, Sade et al. 2014, 2015). Aquaporins in the bundle sheath have recently been shown to regulate leaf hydraulics in Arabidopsis (Shatil-Cohen et al. 2011, Sade et al. 2014, 2015); therefore it is likely they do the same in hybrid poplar leaves.

Extending from the bundle sheath are bundle sheath extensions, parenchymatous extensions that connect the vein to the epidermis (Zwieniecki et al. 2007, Buckley et al. 2011). Bundle sheath extensions have increasingly been linked to hydraulic facilitation, and are believed to be an alternative pathway for water to the epidermis (Buckley et al. 2011, Sack et al. 2015). The

current study will measure both minor vein area (including the bundle sheath) and bundle sheath extension area to determine whether these structures influence hydraulic conductance in hybrid poplars.

1.4 *Populus* genotypes as a study species

Over the past thirty years, *Populus* species *(P. trichocarpa*, *P. balsamifera*, *P. tremuloides*, *P. deltoides*, etc.) and hybrid poplar clones have been increasingly used in commercial plantations and research. *Populus* genotypes are fast-growing, easy to clonally propagate via cutting, and remarkably diverse in phenotypic variation (Bradshaw et al. 2000, Ridge et al. 1986). Poplars are also quick to exhibit physiological responses to environmental conditions and have a tight coupling between morphological traits and biomass productivity (Bradshaw et al. 2000), making them an ideal study subject for carbon-water relations. Lastly, the genus *Populus* has a small and recently sequenced genome (Tuskan et al. 2006) and aquaporin family (Gupta and Sankararamakrishnan 2009, Almeida-Rodriguez et al. 2010). These resources have earned *Populus* nicknames such as "a model forest tree" and the "*Arabidopsis* for Forestry" (Bradshaw et al. 2000, Taylor 2002).

In addition to hybrid poplars, this study will also measure aspen (*Populus tremuloides* Michx.). Aspen, like hybrid poplars, is grown commercially for wood pulp and plays a large role in the aspen parkland ecosystems of western Canada (Schreiber et al. 2011). As aspen tends to be more hydraulically resilient than hybrid poplar clones (i.e. more resistant to cavitation and more water-

use-efficient), it should provide an interesting contrast to hybrid poplars in hydraulic strategies (Schreiber et al. 2011).

Recently, Blonder et al. (2011) looked at leaf hydraulic properties in aspen across a climate gradient and found that physiological variation in leaf density was mitigated by local climate. Leaf hydraulic data on aspen would be an interesting addition to previous studies on tree hydraulic traits in field-grown aspen and hybrid poplar (Schreiber et al. 2011, 2013a, 2013b). Most importantly, aspen and hybrid poplar clones are of great economic importance to northern Alberta, and deepening our understanding of *Populus* hydraulic strategies may provide insight for pulp plantations.

1.5 Experimental objectives

The proposed research covers many aspects of leaf hydraulics in an effort to understand how functional traits influence water flow in *Populus* leaves. Previous research has indicated that leaf anatomy strongly influences hydraulic performance (Aasamaa et al. 2001, Sack and Holbrook 2006, Brodribb et al. 2007, Flexas et al. 2013, Nardini et al. 2014). Furthermore, findings from Schreiber et al. (2015) implied that leaf area has a strong correlation with hydraulic resistance to drought in branches. This study is intended to build upon Schreiber et al.'s (2015) findings by researching important leaf hydraulic parameters in four of the same hybrid poplar clones (GG, NW, OK, and P38).

Through a greenhouse study, I will focus on measuring leaf traits in 6 *Populus* genotypes from northern Alberta that vary physiologically: Aspen (AS), Brooks (BR), Green Giant (GG),

Northwest (NW), Okanese (OK), and P38P38 (P38). These particular genotypes were selected because they demonstrate different hydraulic strategies, ranging between stable (GG, NW, OK) and variable (AS, BR, P38) performance. In this study, performance is defined as hydraulic performance, as quantified by leaf hydraulic conductance (K_{leaf}) and stomatal conductance (gs).

My experimental questions were these:

1. How do physiological proxies of hydraulic performance (K_{leaf} and gs) vary in closely related *Populus* genotypes?

2. What aspects of leaf anatomy correlate with these physiological traits? Are there anatomical proxies for high-performance?

By exploring different functional traits in *Populus* leaves, we may better understand hydraulic constraints on performance.

2 Materials and Methods

2.1 Plant material and growth conditions

2.1.1 Hybrid poplar clones

The plant material used in this study was obtained from Alberta-Pacific Forest Industries Inc© ("Al-Pac"), located near Boyle, Alberta, Canada (54˚49'N, 113˚31'W). Five genetically similar hybrid poplar clones (Table 2.1) were selected for their variable hydraulic properties and growth performance, based on previous studies on the same field-grown poplars (Schreiber et al. 2011, Schreiber et at. 2015).

Clone name	Parentage	Parent gender	Al-Pac field site	GPS Coordinates
Brooks (#1)	*P. deltoides* x *P. x petrowskyana*	Male	Sanftl	54^{0}46'16.6," 113^{0}06'17.6"
Green Giant (or Brooks #6)	*P. deltoides* x *P. x petrowskyana*	Male	Rooke	54^{0}45'47.7," 113^{0}06'04.7"
Northwest	*P. balsamifera and P. deltoides*	Male	Lovelace	54^{0}33'27.1," 113^{0}07'09.2"
Okanese	*P. "Walker"* x *P. x petrowskyana*	Male	Cooper	54^{0}27'50.3," 113^{0}09'24.8"
P38P38	*P. balsamifera* x *P. simonii*	Female	Jones	54^{0}21'02.4," 112^{0}51'03.9"

Table 2.1: Parentage information of the hybrid poplar clones from Al-Pac, sampled from commercial sites planted in 2007. Since hybrid poplars are dioecious, the gender of the parent tree is noted along with the parentage and Al-Pac harvest site. The parent *P. x petrowskyana* is a hybrid cross between *P. laurifolia* x *P. nigra*. *P. "Walker"* is a cross between *P. deltoides* and *P. petrowskyana*.

Side-branch cuttings approximately 15 cm in length were taken in early 2014 from Al-Pac plantation sites for 5 hybrid poplar clones: Brooks (BR), Green Giant GG), Northwest (NW), Okanese (OK), and P38P38 (P38). The dormant parent trees ranged from 5-9 m tall, with an average diameter at breast height of 6.6 cm (Schreiber 2015, Hacke and Campbell, unpublished data). Cuttings were preserved at -18˚C from harvest until planting.

Before planting, a fresh cut was made at the base of each stem before partially submerging in de-ionized ("DI") water. The submerged cuttings were covered with a dark plastic bag and monitored for two days; a method suggested by previous trials with similar hybrid poplar cuttings (DesRochers and Thomas 2003). After soaking, the cut segments were planted in a 64-well Styrofoam block in Sun Shine Mix #4 soil (© 2014 Sun Gro Horticulture Canada Ltd) in the ALES greenhouse under semi-controlled conditions (16/8 light: dark photoperiod; 22 ˚C/18˚C day: night air temperature).

Fertilization occurred once weekly with 2 g L^{-1} of 10:52:10 NPK. Watering took place three times per week until visible roots and bud break had occurred (~3 weeks). Daily watering and weekly fertilizing of 20:20:20 NPK began after bud break, and cuttings were moved into 6" pots.

2.1.2 Aspen seedlings

Aspen (*Populus tremuloides*, AS) seeds were collected around Edmonton, AB by Dr. Simon Landhausser (Department of Renewable Resources, University of Alberta). After germination, the seedlings were watered every other day and fertilized weekly with 10:52:10 NPK. Growth chamber temperature was 21˚/18˚C day: night. The seedlings were thinned and replanted ~6

weeks later into 3.8L pots of Sun Shine Mix #4, and moved to the ALES greenhouse (16/8 light: dark photoperiod; 22 ˚C/18˚C day: night air temperature).

Both hybrid poplars and aspen were grown under the same conditions in the ALES greenhouse until a height of 0.5-1.0 m was reached (hybrid poplars = 12 weeks; aspen = 18 weeks). Plants were arranged in rows on the greenhouse bench according to genotype and moved every 1 to 2 weeks. Environmental conditions in the greenhouse (light, temperature, and humidity) were stabilized as much as possible.

2.3 Physiological measurements

2.3.1 Leaf hydraulic conductance (K_{leaf})

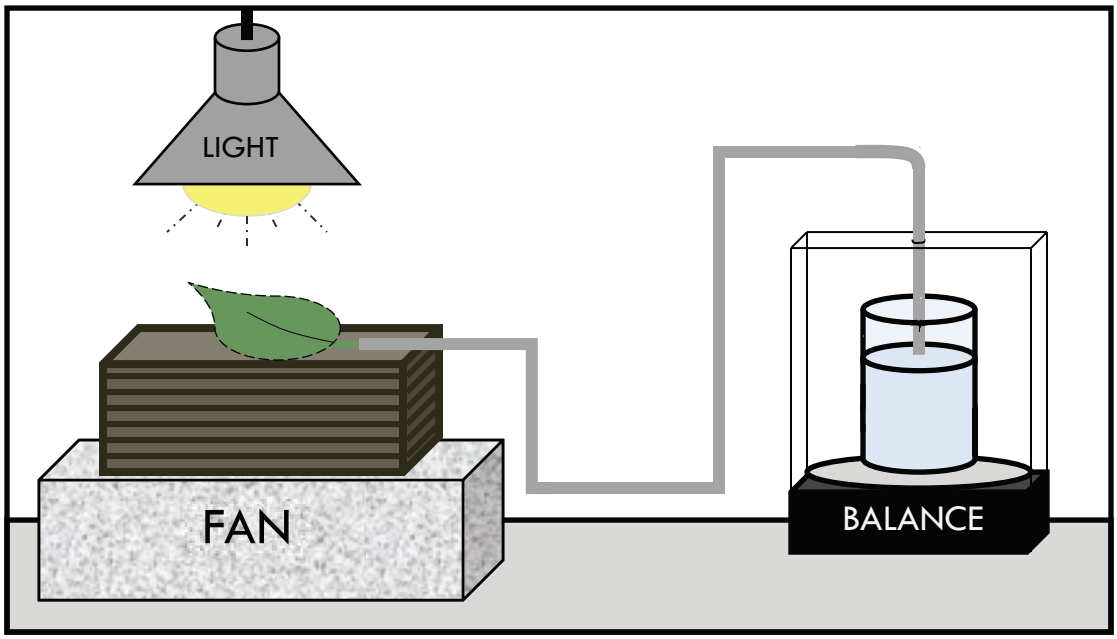

Figure 2.1: Diagram of the Evaporative Flux Method, modeled from the "jOVE" video by Sack and Scoffoni (2012). This method was used to determine maximum leaf hydraulic conductance (K_{leaf}^{max}) by measuring transpiration from the leaf surface, as determined by the amount of KCL solution leaving the balance. The lamp illuminated the leaf from above, while the fan kept the air well-stirred below.

After the poplar cuttings reached 0.5-1.0 meter in height, 8 plants per clone (Brooks, Green Giant, Northwest, Okanese, and P38P38) and 7 for aspen were harvested for leaf hydraulic conductance (K_{leaf}) measurements. Over a period of three weeks, four plants were cut near the stem base stem the night before K_{leaf} measurements were taken. These plants, selected at random, were then placed into dark, humid plastic bags, and transported back to the laboratory. The shoots were re-cut underwater and allowed to rehydrate overnight. A dark plastic bag was placed over top so plants could recover full hydraulic conductivity.

Between 9:00 am and 1:00 pm the following day, the Evaporative Flux Method (EFM) was used to calculate maximum leaf hydraulic conductance (K_{leaf}^{max}; Fig. 2.1). The origin of this method is usually attributed to Boyer (1977), but revision by Sack and Holbrook (2003) and Brodribb and Holbrook (2003) increased the accuracy of the EFM. In the laboratory, the poplars harvested the night before were uncovered and allowed to acclimate to ambient light. One fully expanded leaf in the 8^{th}-9^{th} position from apical meristem was measured per shoot, as determined by the leaf plastichron index (LPI, Larson and Isebrands 1971). This yielded a total of eight leaves per hybrid clone (BR, GG, NW, OK, and P38) and seven for aspen (AS).

The selected leaf was cut underwater at the petiole, then immediately re-cut underwater with a fresh razor blade. Pre-stretched Parafilm M® was wrapped around the petiole to ensure a tight seal with the tubing, which ran from the leaf to a reservoir resting on a balance (model CP 224S, Sartorius, Gottingen, Germany). The reservoir and tubing were filled with filtered 20 mM KCl and 1 mM $CaCl_2$ solution, commonly used to mimic xylem sap (KCl solution; Schreiber et al. 2011, Laur and Hacke 2014). Once the petiole base was secured in the tubing, the leaf was patted dry and placed on the EFM apparatus (see Fig. 2.1). A bright LED light (~1000 µmol m^{-2}

s^{-1} PAR at leaf level, Husky LED Work Light, The Home Depot, Canada) lit the adaxial leaf surface from above, while a fan stirred the air below (Fig 2.1).

Transpiration-driven flow was measured every 30s through a modified Excel sheet (created by L. Plavcová 2013). The leaf remained connected to the system until a stable flow rate ("E") was achieved (~30-60 minutes). If a leaf failed to stabilize after 60 minutes or an air bubble formed in the tubing, the measurement was discarded (Sack and Scoffoni 2012). After steady state flow was reached, the leaf was removed from the tubing and quickly placed into a pressure chamber (Model 1505D, PMS Instruments, Albany, OR, USA) to measure water potential. Lastly, the leaf was scanned for area (EPSON V700 Photo Color Scanner), and preserved in cold formalin-acetic acid for later measurements.

K_{leaf}^{max} was calculated through using the following equation:

$$K_{leaf}^{max} = E/\Delta\Psi_{leaf} \quad (1)$$

Here, K_{leaf}^{max} was calculated for each leaf by dividing steady flow (E, mmol m^{-2} s^{-1}) by the water potential difference across the leaf ($\Delta\Psi_{leaf}$), represented as final water potential (Ψ, MPa; Sack and Holbrook 2006).

2.3.2 Stomatal conductance

Stomatal conductance (g_s) of aspen and hybrid poplar leaves was measured with an AP4 Leaf Porometer (Dynamax Inc, Houston, TX, USA) on the 8th fully expanded leaf on every plant per clone (n=9), between 9:00 am and 1:00 pm. g_s measurements took place both one week and one day before K_{leaf} measurements began, and twice throughout the three-week period following (July 2014). The measurements from July 4th were selected for subsequent data analysis, as they

had been taken one day ahead of K_{leaf} measurements, and had seasonally similar sunlight hours. Additionally, July 4th was the one "complete" data set, as before aspen was not included, and after randomized plants were removed for K_{leaf}. It is important to note that while g_s measurements were conducted on different days, the data showed consistent patterns in genotype ranking and conductance values.

Calibrations were made according to manual directions before measurement in greenhouse conditions (20-22°C, 115µmol m^{-2} s^{-1} PAR, 30% RH). Since hybrid poplar leaves are amphistomatic, the g_s values for both ab- and adaxial leaf surfaces were combined.

2.4 Leaf tissue preparation for microscopy

2.4.1 Leaf preservation

In the morning of the K_{leaf} measurements, one leaf (LPI 7) from each shoot was sampled for preservation between 7:45 and 8:15 am. The leaf was immediately dissected into two parts: a two cm^2 segment containing both midrib and lamina from the bottom third of the leaf, and a one cm^2 section of the petiole (Fig. 2.2). These tissues were chosen to study the petiole, lamina, and midrib, which were believed to represent the major hydraulic pathways in the leaf (Sack and Holbrook 2006).

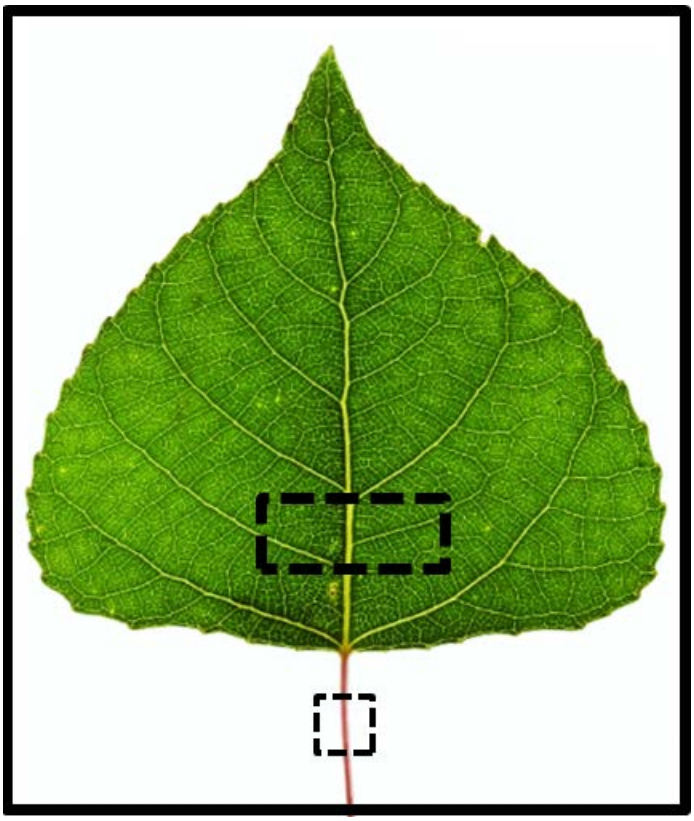

Figure 2.2: Poplar leaf showing tissue sections removed for preservation. Both the lamina and midrib are captured in the top square (1x2cm), while the petiole alone is sampled in the bottom square ($1cm^2$).

The tissue was preserved for microscopy based on a modified protocol of Berlyn and Miksche (1976), as described in Almeida-Rodriguez et al. (2011). According to the protocol, the cut tissue was immediately transferred to 25 mL glass vials (Fischer Scientific) of 4˚C FAA (formalin acetic acid: 500mL of 100% ethanol, 50mL glacial acetic acid, 100mL of formaldehyde, and 350mL of phospho-buffered saline (PBS) per liter) and gently inverted several times. The FAA was replaced with fresh solution after 30 minutes, and removed completely after incubation at 4˚C overnight. After rinsing twice with 10x PBS for 30 minutes,

the leaves were brought to 70% ethanol through a dilution series. The vials were stored at 4˚C to be used for subsequent anatomical measurements (personal communication with J. Laur).

2.4.2 Leaf clearing and staining

To chemically remove the mesophyll tissue from the leaves, a modified protocol from Berlyn and Miksche (1976) was used, authored by Scoffoni and Sack (2013). An ethanol dilution series gradually brought the leaves previously measured for K_{leaf} to E-Pure water. Five percent sodium hydroxide (NaOH) in E-Pure water was applied and left for 5-9 days, the duration determined by the size of the leaf. Once the leaf was sufficiently transparent, the 5% NaOH was poured off and replaced with E-Pure water.

To visualize the vein orders present in the leaf, both safranin and fast green dyes were used. Leaves were prepared for staining through another ethanol dilution series. The leaf was then immersed in a 0.1% concentration of safranin (1g safranin for 1000mL EtOH), resting for 1 minute before moving to 100% EtOH to remove excess dye. Next, the leaf was placed into a 0.1% beaker of fast green, agitated for 30s, and moved to 100% EtOH. A reverse dilution brought the stained leaf back to E-pure water. The leaf was mounted on transparency film (CG5000; 3M Visual Systems Division) and scanned at high resolution (Scoffoni and Sack 2013).

2.4.3 Preparation for light and confocal microscopy

8 μm sections of the midrib and petiole were embedded in paraffin blocks, sectioned, stained, and mounted on slides for light microscopy imaging. Images were taken with a digital camera (DFC420C, Leica, Wetzlar, Germany) attached to a light microscope (DM3000, Leica) at 25-

400x for different regions of interest in the leaf. Measurements of mean vessel diameter in petioles, minor vein area, bundle sheath extension area, distance between the xylem and lower epidermis, and lamina thickness were hand-traced using ImagePro software (Image-Pro Plus 6.1; Media Cybernetics, Silver Spring, MD, USA). These particular traits were chosen as previous research suggested a correlation with hydraulic traits in leaves (Sack et al. 2003, Zwieniecki et al. 2007, Schreiber et al. 2011, Nardini et al. 2014).

2.5 Anatomical measurements and microscopy

2.5.1 Leaf vein density

Vein orders for *Populus sp*. leaves were determined based on the Manual of Leaf Architecture (Ellis et al. 2009). Vein density (mm mm^{-2}) was calculated by manually tracing vein length (mm) and dividing by area of interest ("AOI", mm^2) with ImagePro software. Primary (1˚) and secondary (2˚) vein densities were measured for the entire leaf, and corrected by total leaf area. Tertiary (3˚), quaternary and higher (4˚+) veins were averaged from three sections of the leaf (Fig. 2.3), and corrected by their respective AOI area. Images were taken at 40x on a stereomicroscope (MS5; Leica, Wetzlar, Germany).

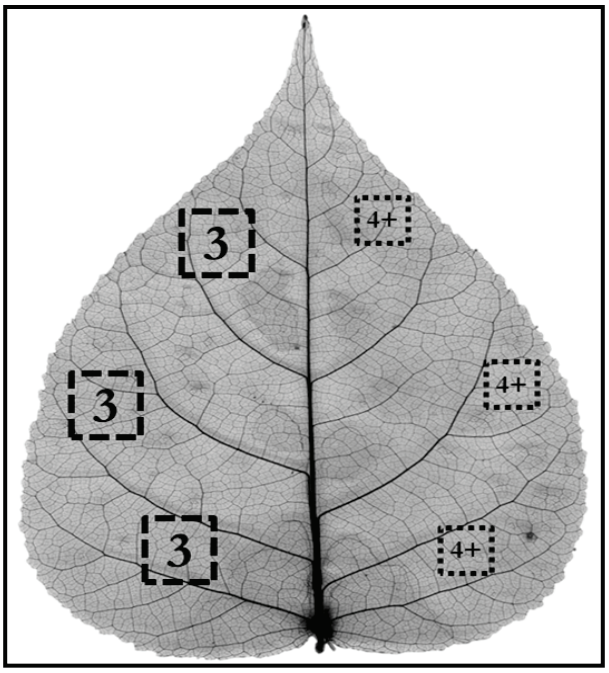

Figure 2.3 A cleared Green Giant leaf, showing vein orders and sub-sections measured for vein length per area (VLA). The midrib (primary) vein extends vertically from the leaf base, while the secondary veins branch off at ~45° angles. The larger squares ("3") represent the sub-sections taken for tertiary vein measurements, and the "4+" squares depict those for quaternary and higher vein measurements. These length measurements were divided by either leaf area (primary and secondary) or by sub-section area (tertiary and higher) to calculate VLA.

2.5.2 Anatomical measurements

Petiole cross-sectional area (A_p) and total xylem area in the petiole (A_x) were measured from 25x and 100x images, respectively, of the slides prepared above (section 2.4.3; see Fig. A1). The diameter of the xylem vessels in the petiole (A_x) was measured using ImagePro software.

Lamina thickness (T_{Leaf}) was measured from 25x images for all hybrid poplar clones. As aspen had a much thinner lamina, it was necessary to measure thickness at 100x magnification. Six measurements per leaf were averaged to encompass the margin and middle of the leaf lamina.

Bundle sheath extension area (A_{BSC}), vein area (A_v), and distance from xylem to lower epidermis ($D_{L.epidermis}$) were all measured at 200x (hybrid clones) or 400x (aspen; see Fig. 3.8). The $D_{L.epidermis}$ was measured by tracing cell walls to estimate the apoplastic path length of water leaving the xylem to the lower epidermis (see Fig. 3.8).

Side veins were selected by the following criteria: size (2,500 to 15,000 μm^2), discernible xylem vessels and bundle sheath cells, and bundle sheath extensions reaching both the ab- and adaxial edge of the lamina. All measurements (n=30 per clone) were hand-traced using ImagePro software (see Figure 3.5)

2.5.3 Theoretical petiole conductivity

I used the Hagen-Poiseuille equation to calculate theoretical conductivity of the petiole (*"*$K_{h.petiole}$"). This equation, originally created to explain capillary flow, has been shown to appropriately estimate flow through vessel elements and tracheids in trees. By using this equation (2), we can theoretically estimate petiole conductivity (3) in cases where measurement is impossible. In equations (2) and (3), D_v represents the hydraulically weighted vessel diameter, "n" equals the number of vessels, "p" and "η" stand for the density and viscosity of water (998.2 kg m^{-3} and 1.002 x 10^{-9} MPa s, respectively), and "*d*" represents vessel diameter (Schultz and Matthews 1992, Tyree and Zimmerman 2002).

$$D_v = \left(\frac{(\sum d^4)}{\eta} \right)^{1/4} \quad (2)$$

$$K_{h.petiole} = (\pi \sum d^4)/128\eta \quad (3)$$

It is important to note, however, that the calculated $K_{h.petiole}$ values are often two to three times larger than actual conductivity (Schultz and Matthews 1993, Sperry and Pockman 1993). This is largely due to the hydraulic resistance of pit membranes and perforation plates, unaccounted for by the 'perfect cylinder' assumed by the Hagen-Poiseuille equation (in 1.3.3; Tyree and Zimmerman 2002).

2.6 Statistical analysis

Statistical analysis was carried out using SigmaPlot Version 13.0 (Systat Software, San Jose, CA) and the R-Programming Environment (R Development Core Team 2013). Tests for normality and equal variance were performed using the R functions *shapiro.test* and *bartlett.test*. The package *Hmisc* (Harrell 2015) was used to calculate the Pearson's correlation coefficients and their significance.

A one-way analysis of variance (ANOVA) was performed on the dependent variables leaf hydraulic conductance, leaf area, and stomatal conductance, using SigmaPlot 13.0 to determine significant differences between the means of *Populus* genotypes. Significant main effects were followed with Tukey-adjusted pairwise comparisons, as I wanted to detect differences between individual genotype means. This analysis was carried out as a randomized complete block design, where "day of measurement" was considered the block effect to reduce the residual variance. No significant differences between blocked and unblocked analysis emerged for leaf hydraulic conductance, leaf area, and stomatal conductance, from which I concluded that these parameters were not influenced by the measurement date.

3 Results

3.1 Morphological differences

Figure 3.1 illustrates the existing differences in leaf shape and size among hybrid poplar clones and trembling aspen. *Populus* leaves are characterized by several morphological traits shown here: a deltoid (P38) or lanceolate (Okanese) shape, a wavy leaf margin (Brooks), and pointed "teeth" at the margin edge (Brooks, Okanese, Northwest; Settler 1998). Leaves are all from LPI 8 (Larson and Isebrands 1971).

As shown in Fig. 3.2, the *Populus* leaves fell into three distinct groups in terms of leaf area: small (P38 and aspen), medium (Brooks, Okanese, and Green Giant), and large (Northwest). Variation in leaf size impacted numerous other traits, including major vein density, petiole cross-sectional area, xylem area in the petiole, and stomatal conductance (Table A3).

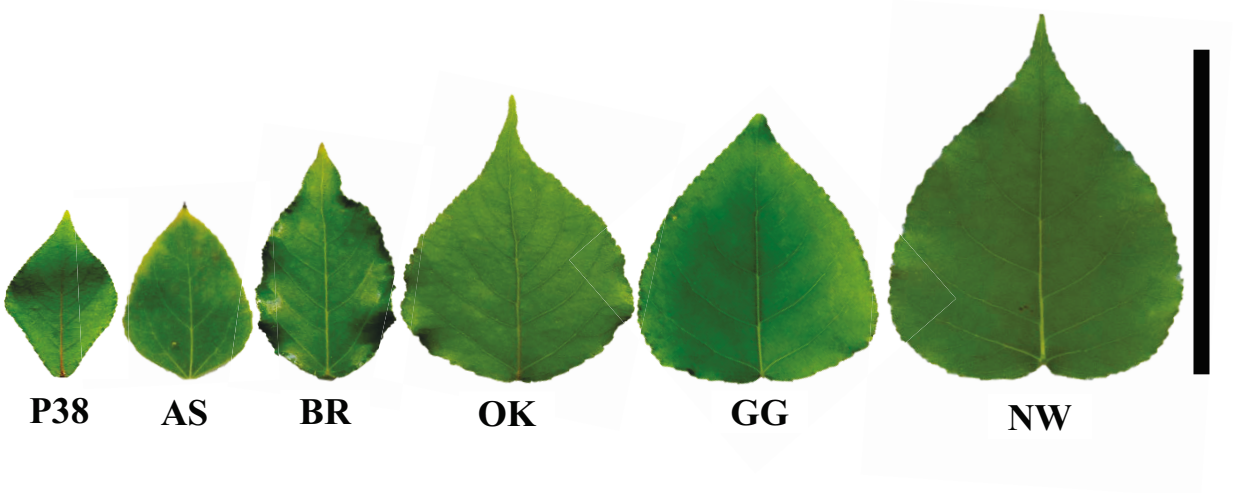

Figure 3.1: Leaf morphology of trembling aspen (AS) and five hybrid poplar clones. The order of leaves is determined by leaf size. The following hybrid poplar clones were included in the analysis: P38P38 (P38), Brooks (BR), Okanese (OK), Green Giant (GG), and Northwest (NW). Scale bar = 10 cm.

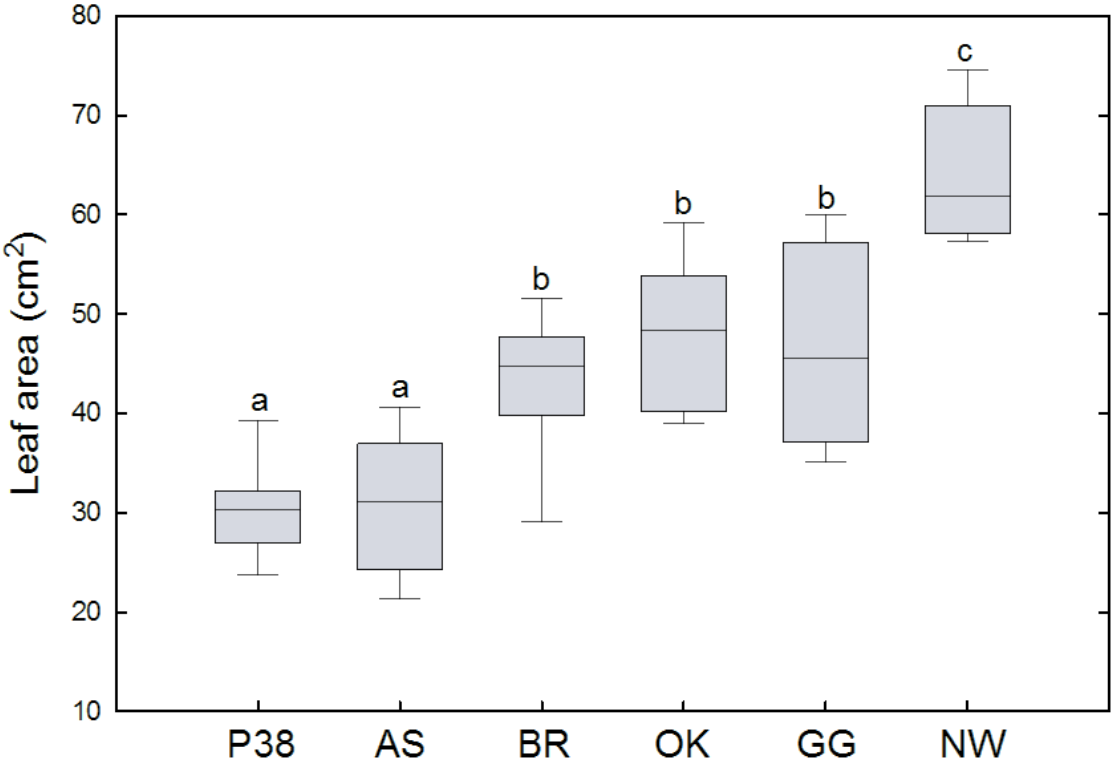

Figure 3.2: Box plot showing variation in leaf area among *Populus* sp. (abbreviations same as Fig. 1). Median of the data is represented by the black line within the shaded box. Whiskers represent 10% (lower) and 90% (upper) percentiles. Box limits on either side of the median represent 25% (lower) and 75% (upper) percentiles. Leaf areas same as those measured for leaf hydraulic conductance (n=7 for AS, n=8 for P38, BR, OK, GG, NW). Letters indicate significant ($P \leq 0.05$) differences between genotypes, as determined from a Tukey post-hoc test / One-way ANOVA.

3.2 Relationships between leaf area and hydraulic structures of the leaf and petiole

Major vein density (also known as major vein length per area, VLA_{major}) was negatively correlated with leaf area (A_L). Here, I define major vein density as the cumulative density of primary and secondary veins. Interestingly, this trend was not only apparent across the hybrid poplar clones (Fig. 3.3a), but also within each genotype (Fig. 3.3b). This pattern was very strong for the five hybrid poplar clones ($r^2 = 0.93$, $P = 0.03$), as the solid regression line in (a) shows. With aspen included, the trend was not significant (dashed line; $r^2 = 0.47$, $P = 0.15$). Results from statistical analysis (coefficients and significance values) are displayed in Table A3.

Figure 3.3b displays the VLA_{major} relationships within each genotype. A grouping of Okanese, Green Giant and Northwest was apparent, while individual leaves of P38 and Brooks also showed considerable overlap. Aspen, by contrast, remained isolated (Fig. 3.3a, b).

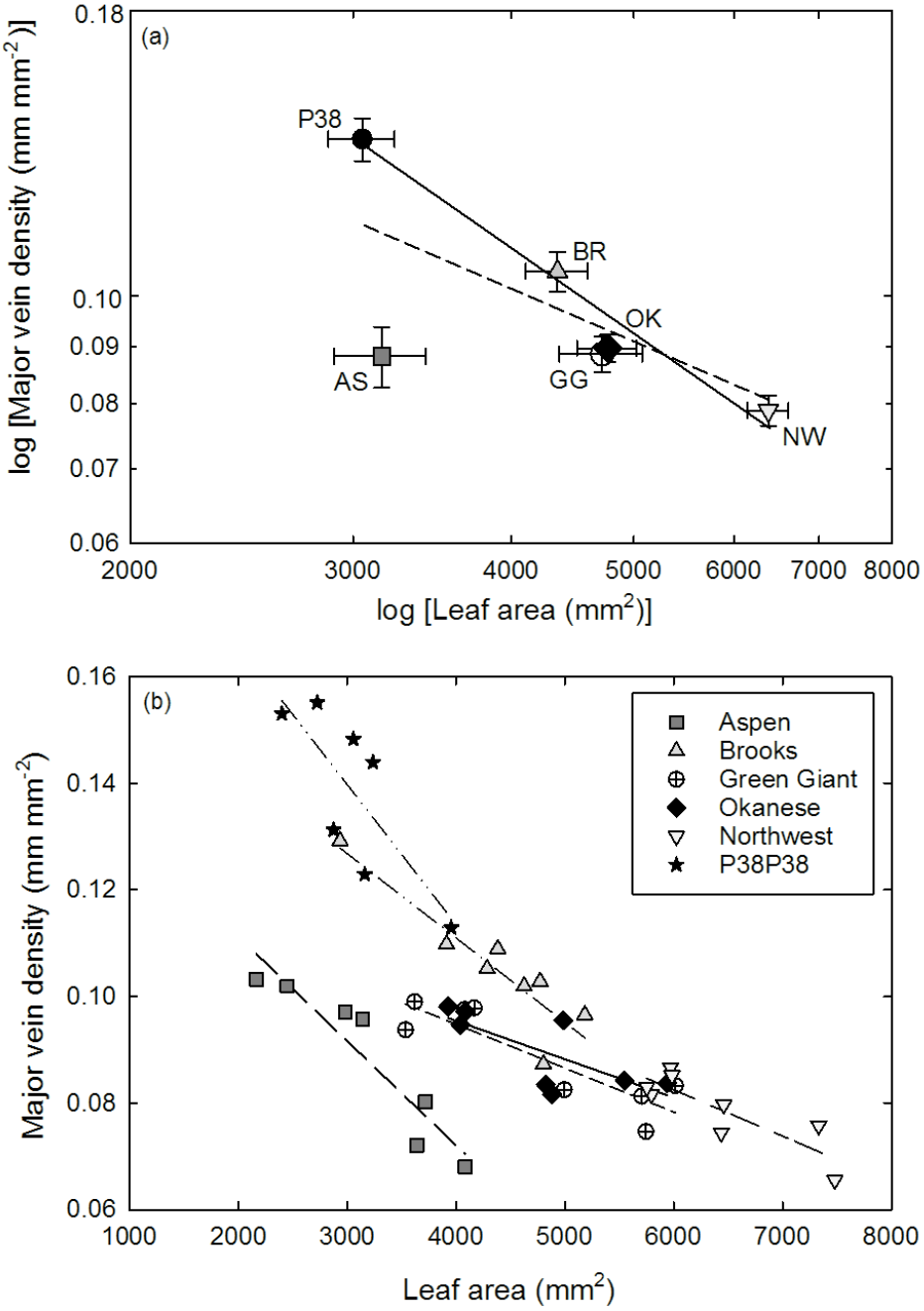

Figure 3.3: (a) Log-log plot showing scaling of major vein density (density of primary + secondary veins) and leaf area (A_L). Acronyms for genotypes given in Fig. 1. Genotype means with error bars (±SEM) are displayed in (a). Linear regression analysis gives an r^2 value of 0.47 with aspen (dashed line), and 0.93 without (solid line). (b) Scaling of major vein density and leaf area within each genotype.

The cumulative xylem area in a petiole cross section was correlated with several traits including leaf area and stomatal conductance (Fig. 3.4, Table A3). Significant relationships were found between both of these properties, at values of $P \leq 0.05$ and 0.01, respectively. The hybrid poplar Northwest had the largest amount of xylem area, which correlated with large leaf area and high stomatal conductance (both ad- and abaxial).

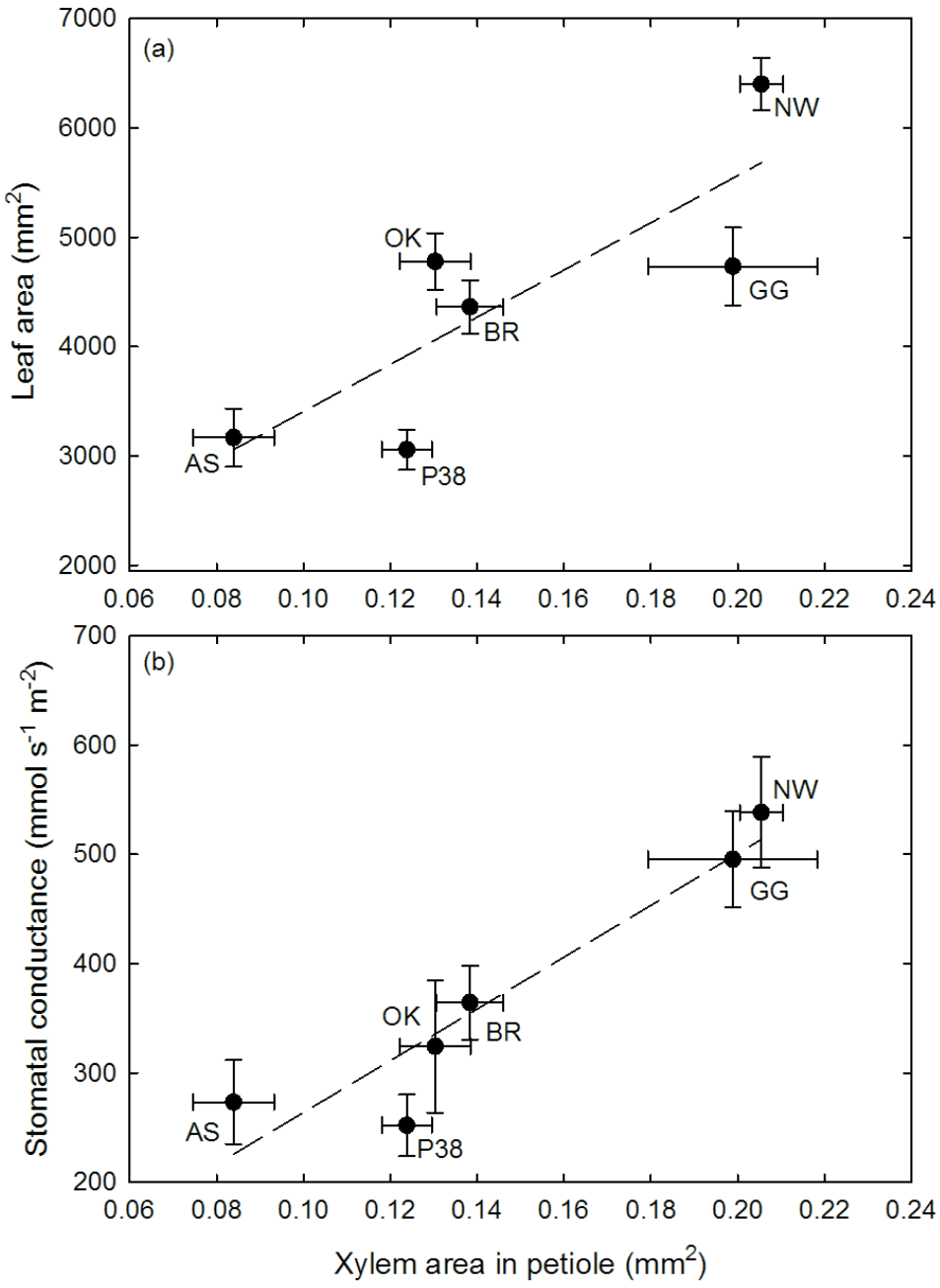

Figure 3.4: Leaf area (a) and stomatal conductance (b) as a function of the cumulative xylem area in petiole cross sections. The r^2 values from a linear regression are 0.68 (a) and 0.89 (b), indicating a strong relationship between the amount of xylem in the petiole and the water flow it can support. Without aspen, the r^2 values are 0.57 (a) and 0.95 (b).

In Figure 3.5, stomatal conductance showed a particularly strong correlation with the theoretical 0.99, $P \leq 0.001$). When aspen was included, the correlation was weaker, but still significant (r^2 = 0.85, $P \leq 0.009$).

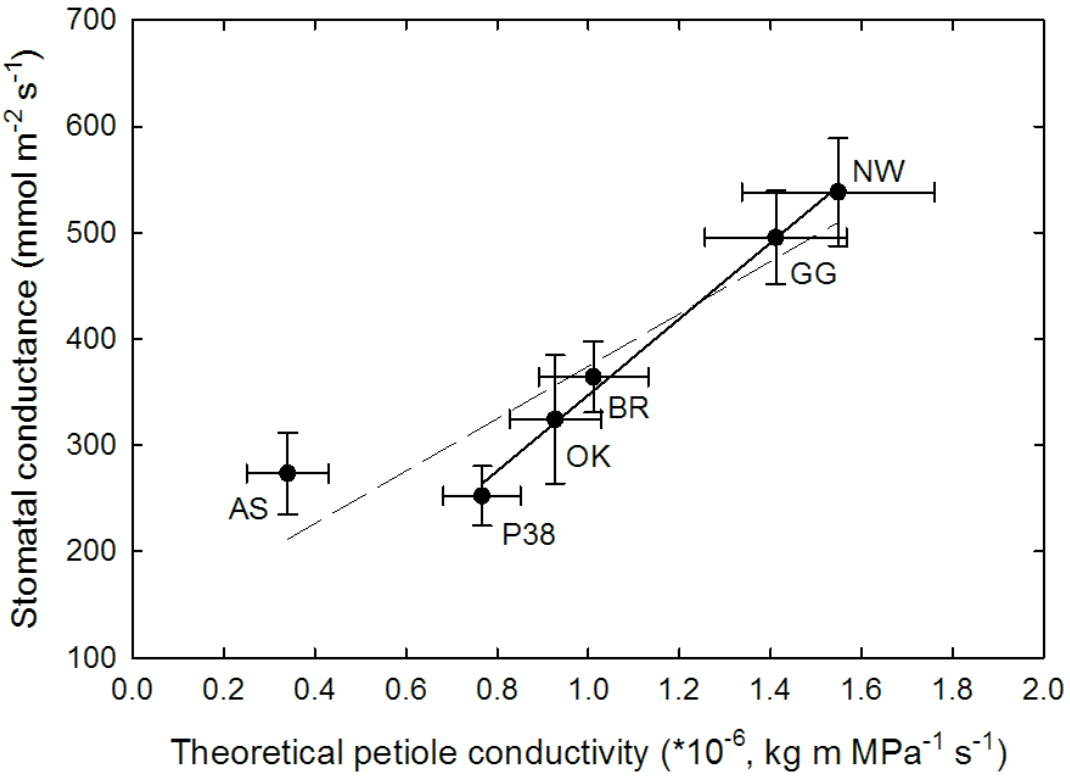

Figure 3.5: Theoretical petiole conductivity, calculated from the Hagen-Poiseuille equation (section 2.4.4). Strong positive correlations were found, both with (r^2 = 0.85, dashed line) and without (r^2 = 0.99, solid line) aspen.

3.3 Interactions in leaf extra-xylem anatomy

Anatomical differences between genotypes are explored further in Figure 3.6. These three poplar genotypes (aspen, Green Giant, and Northwest, in order) were chosen because they exhibited striking differences in anatomical traits. While the arrangement of vascular bundles in the petiole varied between genotypes (Fig. 3.6a-c), the amount of xylem area remained proportional to the petiole cross sectional area in each genotype (Figure A1, A2).

Vessel diameters in the petiole were relatively small in aspen (Fig. 3.6d), compared to the relatively larger fraction in Green Giant and Northwest vascular bundles (Fig. 3.6e-f). The mean diameter values are presented in Table A2.

Perhaps most striking of all is the difference in lamina thickness between leaves (Fig. 3.6g-i). Leaves of the clone Northwest had nearly twice the thickness of aspen leaves. Most of these differences were driven by the spongy mesophyll layer, which varied in thickness more than two-fold across genotypes (Table A2). These differences appeared to coincide with the size of individual cells in the spongy mesophyll, i.e. uniformly small in aspen, and considerably larger in Green Giant and Northwest (Fig. 3.6g-i). In all genotypes, the palisade parenchyma ("PP") consisted of two cell layers; the thickness only varying between 72 μm (aspen) and 103 μm (Okanese; see Table A2).

Hydraulic function may also be influenced by minor vein density (shown in Fig. 3.6j-l). This trait was relatively variable with Green Giant (k) having a lower minor vein density than aspen and Northwest (Table A2).

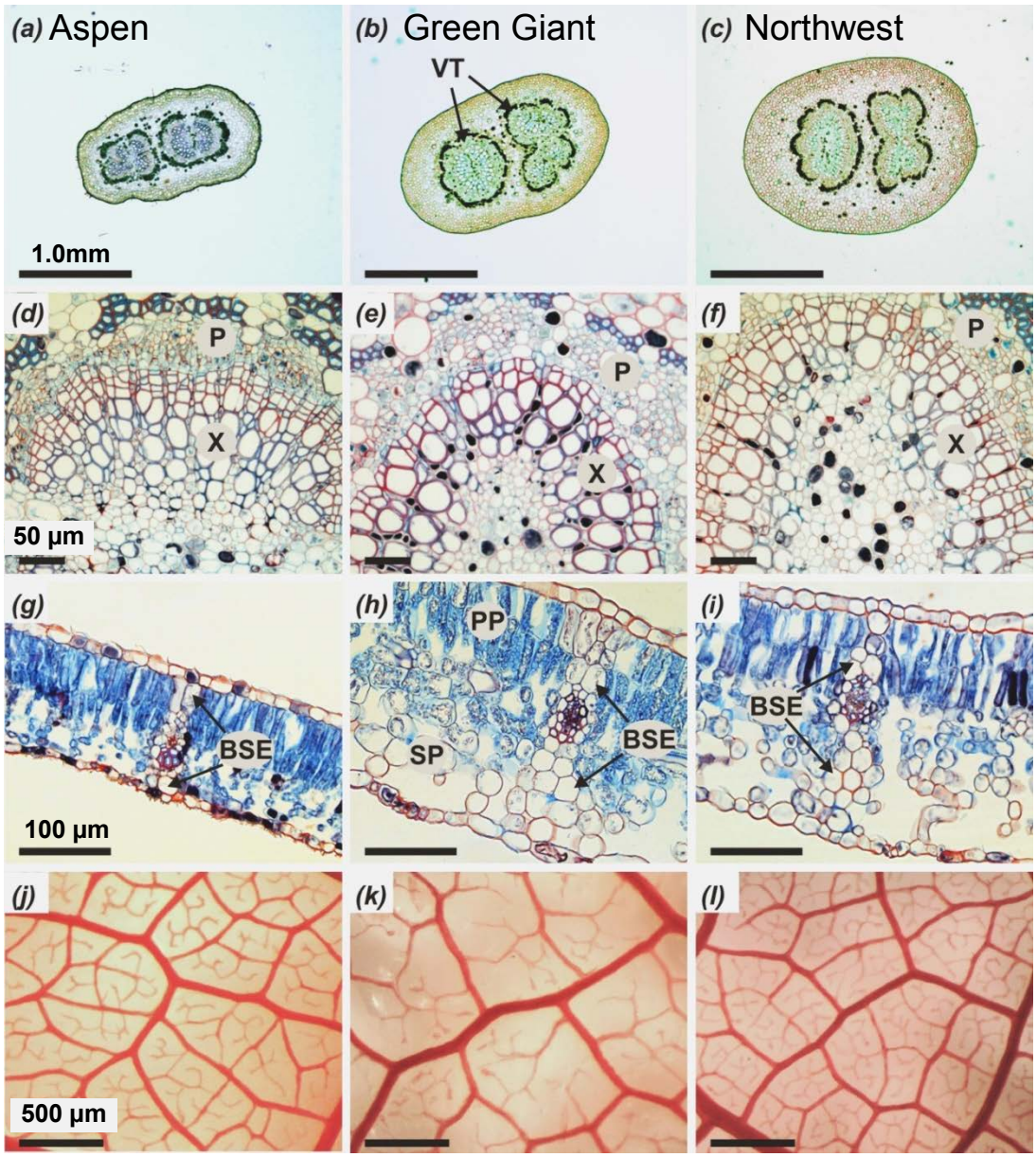

Figure 3.6: Aspects of leaf anatomy in trembling aspen (a, d, g, j), Green Giant (b, e, h, k), and Northwest (c, f, i, l). Images (a) – (c) are petiole cross-sections with the vascular tissue ("VT") present (scale bar = 1.0mm). Images (d) – (f) are cross-sections of the petiole vascular bundle, with the xylem ("X") and phloem ("P") visible (scale bar = 50µm). Sections (g) through (i) show a minor vein in the leaf lamina, in which the palisade parenchyma ("PP"), spongy mesophyll ("SP"), and bundle sheath extensions ("BSE") are visible (scale bar= 100µm). Lastly, images (j) to (l) represent subsections of cleared leaf tissue, with minor veins (tertiary veins and higher) present (scale bar= 500µm). All sections stained with safranin (red) and fast green (blue).

Except for the largest (mid-vein) and smallest veins, all vein orders were associated with bundle sheath extensions (BSE). Most of the BSE cells were relatively large, approximately round, and occasionally had chloroplasts. BSE cells were densely packed, with only small intercellular spaces between them. Cell walls were relatively thin and only lightly stained by safranin. Since BSEs were potentially a large component of extra-xylem hydraulic movement, I was interested in the ratio between BSE area and the veins they projected from (Fig. 3.7 and 3.8a-b).

These measurements revealed that the cross-sectional area of bundle sheath extensions was proportional to the area of the associated veins. A positive correlation was found across genotypes (Fig. 3.7a), albeit strongly influenced by aspen. Fig. 3.7b shows individual data points for each genotype (n=30 for veins and associated BSEs per genotype). Within the hybrid poplar clones and aspen, vein area was positively correlated with BSE area. As seen before (Fig. 3.3), Green Giant and Okanese leaves displayed overlap and similar scaling relationships. Veins and BSEs of aspen leaves tended to be smaller than those of hybrid poplars; hence aspen occupied a unique space in the scatter plot (Fig. 3.7b).

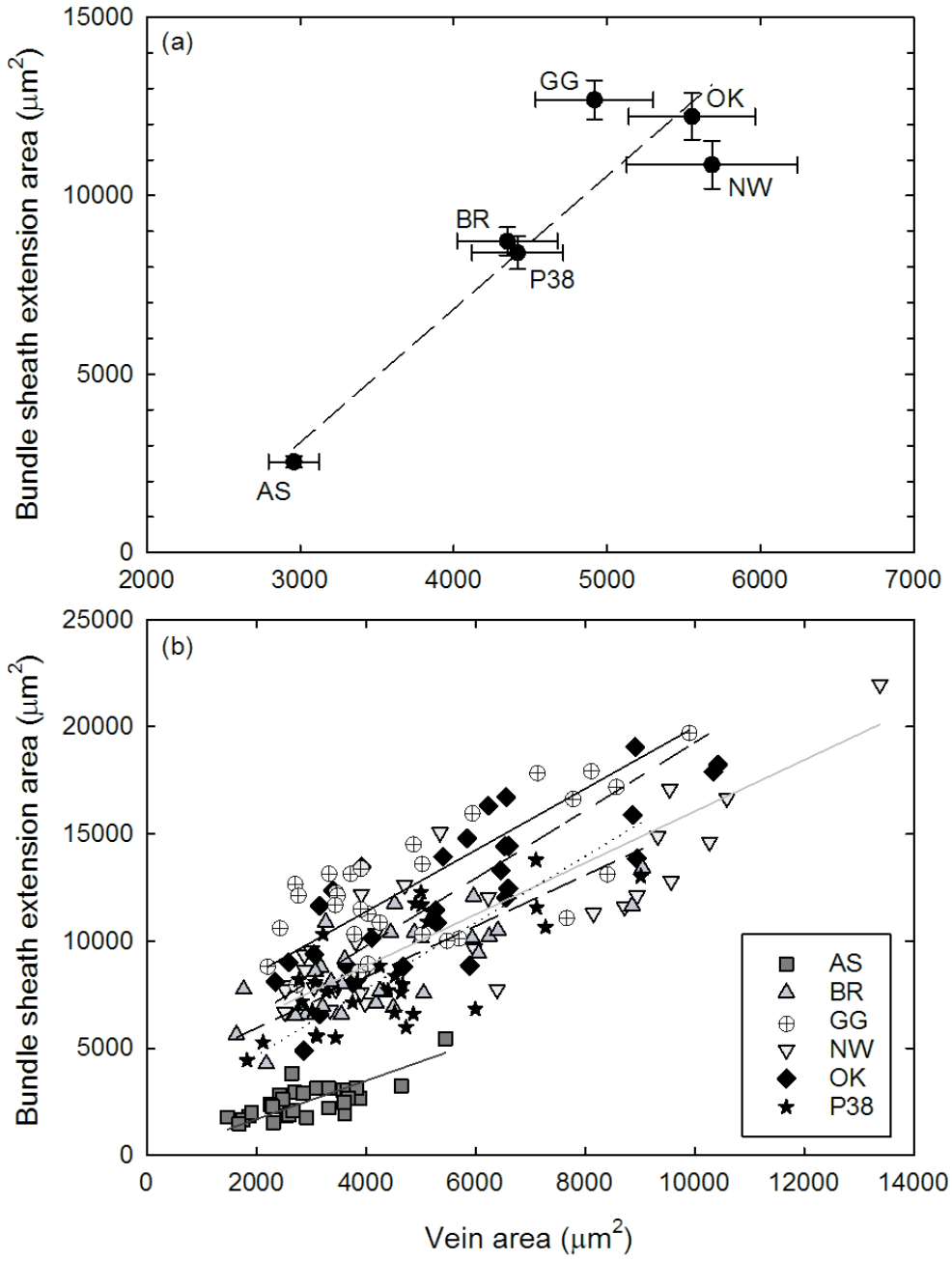

Figure 3.7: Linear relationship between the cross-sectional area of minor veins ($A_{minor.vein}$) and their associated bundle sheath extensions (A_{BSE}). This pattern was apparent within each *Populus* sp. (b), as well as across all genotypes (a). Figure (a) displays mean values of $A_{minor.vein}$ and A_{BSE}, with ±SEM (n=30 per *Populus* sp) for each genotype. Aspen was clearly different from the hybrid clones, though it presented a striking trend when included in the linear regression (a) – an r^2 value of 0.99 ($P \leq 0.05$) with aspen, as compared to 0.49 (P =0.21) without (regression not shown).

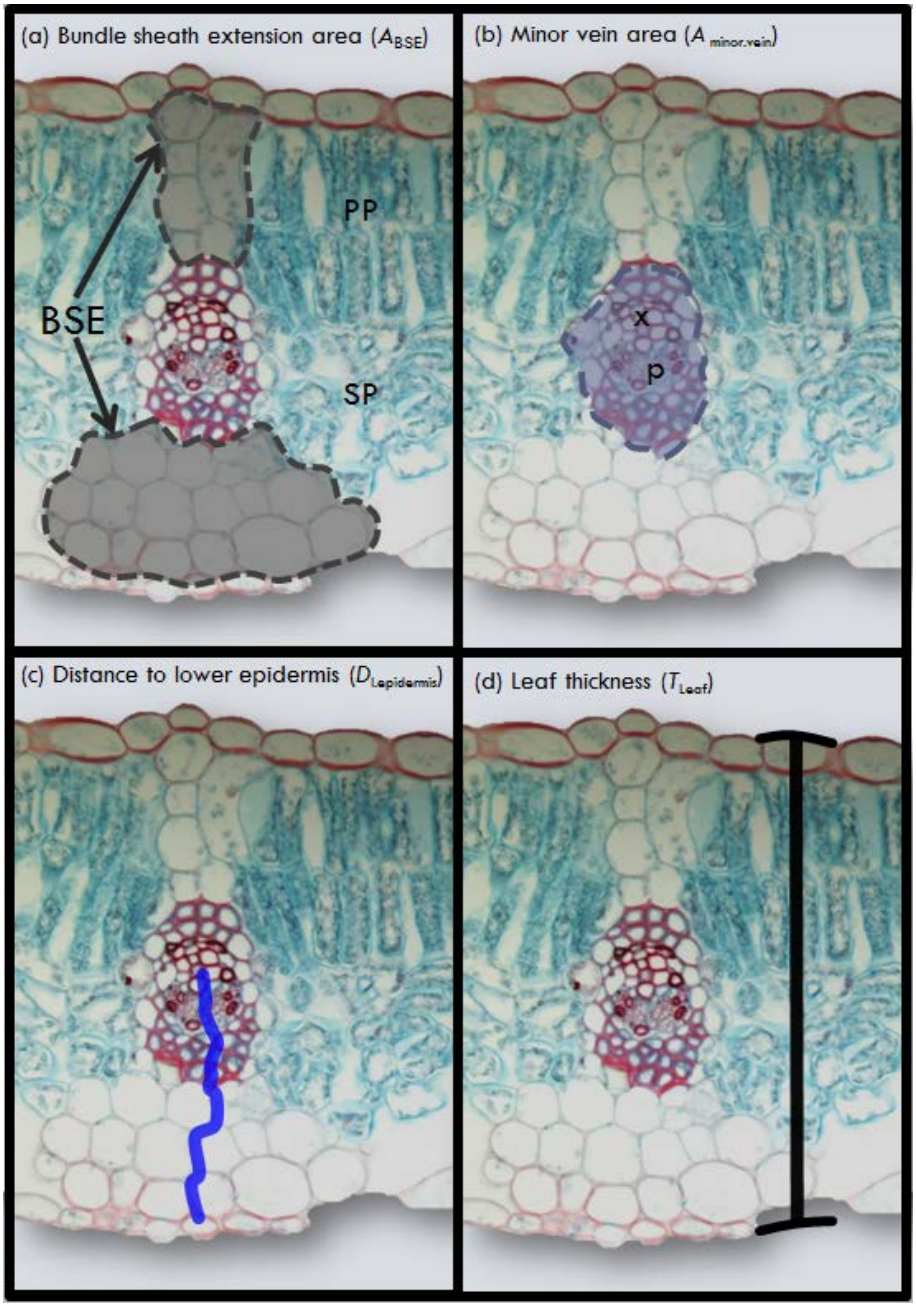

Figure 3.8: Leaf lamina sections illustrating how bundle sheath extension area (a), vein area (b), distance to lower epidermis (c), and lamina thickness (d) measurements were made. Here, "BSE" refers to bundle sheath extensions, "PP" to palisade parenchyma, "SP" to spongy mesophyll, "x" to the xylem, and "p" to phloem. Cells within the gray area (a) represent BSEs, while the purple area in (b) encompasses minor vein area (including bundle sheath cells). The gray BSE areas in the PP and SP layers were added to give the total BSE area per associated vein. Sections were taken from an Okanese leaf.

4 Discussion

Results from this study suggest that key anatomical traits drive patterns seen in *Populus* leaves. Leaf area was the most prominent trait, and correlated strongly with both anatomy (major vein density and petiole xylem area) and physiology (stomatal conductance and theoretical petiole conductivity). However, no anatomical traits correlated with leaf hydraulic conductance.

Aspects of petiole anatomy had the strongest correlation with leaf size and performance. Our findings indicate that petiole hydraulic structure might have a greater influence on leaf hydraulic performance than previously believed.

4.1 Variations in leaf size among *Populus* clones and aspen

One experimental question of this study asked whether anatomical proxies of performance existed in hybrid poplar clones. My results add to recent research in this field; namely, that leaf area is an important parameter to hydraulic performance (Schreiber et al. 2015). Leaf area has previously been shown to positively correlate with height, diameter, biomass, stem volume, vessel diameters, and vulnerability to cavitation in hybrid poplars (Orlovic et al. 1998, Ridge et al. 1986, Schreiber et al. 2015). From this, it can be concluded that leaf area is tightly linked to hydraulic movement and performance.

In Figures 3.1 and 3.2, it is immediately evident that leaf area varies significantly across hybrid poplars and aspen. This finding agrees with a recent study (Schreiber et al. 2015), which looked at variation in hydraulic and anatomical properties of branches of field-grown hybrid poplar clones (Green Giant, Northwest, Okanese, and P38P38). Schreiber et al. (2015) found that leaf

area positively correlated with branch vessel diameter and vulnerability to cavitation in current and 2-3 year-old year shoots, meaning that clones with larger leaves (Green Giant) had wider vessels and a more vulnerable xylem than clones with smaller leaves (P38). Results from our greenhouse study display similar rankings for leaf area and vessel diameter (Table 3.2), illustrating two different strategies for rapid growth. Green Giant, with large leaves and large vessels, is able to move greater amounts of water and support a high rate of stomatal conductance and K_{leaf} (Table 3.2). However, these characteristics might increase xylem vulnerability to drought or freezing-induced cavitation (Davis et al. 1999, Pittermann and Sperry 2003, Schreiber et al. 2013). Therefore, Green Giant might thrive in one growing season but experience severe die-back over the winter.

P38 has previously shown cavitation-resistant xylem at boreal planting sites, indicated by reduced native embolism and percent loss of hydraulic conductivity (Schreiber et al. 2013). P38 grown in the greenhouse had relatively smaller vessel diameter and leaf area, agreeing with previous studies (Schreiber et al. 2011) and the established "smaller is better" trend in leaf shape (Sack et al. 2012, Nardini et al. 2014). I expected P38 to be conservative regarding other leaf parameters, but P38 had the highest K_{leaf} and final height among the *Populus* genotypes, which suggests P38 is able to meet hydraulic demand. However, P38 had one of the lowest stomatal conductance values relative to other clones.

While confusing, I believe these contrary hydraulic strategies perhaps reflect differences in stomatal regulation. Recent research has shown that *P. simonii* x *balsamifera* (P38) showed greater stomatal sensitivity and was more drought-avoidant than other poplar clones (Almeida-

Rodriguez et al. 2010, Arango-Velez et al. 2011). Potentially, this hybrid poplar clone is able to maintain hydraulic integrity of the water column, and is thus able to support higher rates of K_{leaf}.

Overall, these findings show the high degree of inter-clonal variation seen among hybrid poplar clones (Orlovic et al. 1997, Ridge et al. 1986, Ceulemens et al. 1990, Schreiber et al. 2011, 2013, 2015, Hacke 2015). This high degree of variation makes establishing an anatomical proxy of high performance in *Populus* genotypes challenging, and more research investigating the degree of phenotypic plasticity in poplar clones is needed before such a proxy can be established.

4.1.1 Aspen vs. hybrid poplars

In Table 3.3, we see two sets of correlation coefficients and significance values reported: with aspen (white), and without aspen (gray). After analyzing the data, aspen (*P.tremuloides*) appeared to be following a different physiological pattern than the hybrid poplar clones (BR, GG, NW, OK, and P38). Aspen is a visual outlier in almost all figures (Fig. 3.3a, 3.5, 3.6a, d, g, j, and 3.7a). Since aspen was often characterized by small values of anatomy and performance, this discrepancy between aspen and the hybrid poplars sometimes resulted in a positive correlation across the 6 genotypes (Table A3 italicized values, Figure A1). Often, trends that were strongly correlated with aspen were weaker or even ceased to be significant when aspen was excluded (see Fig. A3).

The aspen grown in this study had several physiological differences that may explain the discrepancy between it and the hybrid poplar clones. In contrast to the hybrid poplar clones, aspen plants were grown from seed (2.1.2). This would mean that aspen had neoformed leaves

(from seed), while the hybrid poplars had leaves expanding from a previously dormant bud (likely a combination between preformed and neoformed growth). In addition, aspen leaves were thinner (Fig. 3.6), smaller, and had stomata on the underside of the leaf only (Table A2). The aspen plants also exhibited greater sensitivity to temperature stress in the greenhouse, and appeared to have more anthocyanin pigments in their leaves than the hybrid poplars. The hybrid poplar clones were also genetically more similar to each other than aspen and shared at least one parent (usually *P. balsamifera*, Table 2.1).

However, both aspen and hybrid poplars are important commercial trees to northern Alberta. Aspen was initially chosen for this reason, and because it exhibits a different hydraulic response to drought than hybrid poplar clones (Almeida-Rodriguez et al. 2010, Schreiber et al. 2011). While it proved to be quite different from the poplar clones, aspen still tells an interesting story about hydraulic strategies in *Populus* leaves.

4.2 Leaf area scaling patterns and implications on leaf anatomy

4.2.1 Development of major and minor veins

Leaf area also had a strong correlation with major vein density (VLA_{major}), as we see in Figure 3.3. This significant trend was previously seen across 485 dicotyledonous species (Sack et al. 2012), but only a few studies to my knowledge have focused on leaf architecture within a species or genus (specifically Blonder et al. 2013, Nardini et al. 2014, Xiong et al. 2014, Caringella et al. 2015). Interestingly, a strong trend is seen on a log-based scale at the species/genotype level (a),

as well as within a single genotype (b). From this, it appears that the relationship originally described by Sack et al. (2012) may also occur within a single species/genotype.

In interpreting Figure 3.3, it is clear that major veins are strongly linked to the leaf lamina and the leaf hydraulic pathway. Major veins are responsible for transporting water from the petiole into the leaf, providing mechanical and hydraulic support, and transporting sugar and hormones to the other plant organs (Blonder et al. 2011, Scoffoni et al. 2011, Sack et al. 2012). As mentioned in section 1.2.2, major veins also deliver water for the lamina, which supports both photosynthesis and transpiration. There are functional benefits to leaves with a high VLA_{major}: lamina ratio, including greater tolerance to midvein damage (Sack et al. 2008, Scoffoni et al. 2011) and reduced hydraulic vulnerability (Scoffoni et al. 2011). In *Populus* genotypes, this ratio suggests that despite the similar leaf area, P38 would likely be more resistant to drought and embolism than aspen (Fig. 3.3a).

Yet why is this negative relationship between major vein density and leaf area so prevalent? Current research suggest that a developmental reason drives the trend; namely, the differing rates of early leaf and vein development in the shoot apical meristem. Leaf expansion is slow in early development (primary morphogenesis, section 1.2.2) when major veins are created (Scarpella et al. 2010, Sack et al. 2012). This initial slow period is followed by a rapid phase of cell expansion, when the leaf lamina expands and minor veins develop (Scarpella et al. 2012, Sack et al. 2012, Carins-Murphy et al. 2014).

Importantly, this suggests that the major veins (formed during primary morphogenesis) are subsequently pushed apart during the rapid, leaf expansion phase. The strong relationship

between major vein density and leaf area within a genus (Fig 3.3) is consistent with the above model, and points to developmental constraints on major vein density.

As for minor vein density, no significant correlations emerged with leaf anatomical parameters (Table 3.3). Specifically, no correlation was seen between minor vein density and K_{leaf}, which was one anatomical correlation previously seen to correspond to photosynthesis (Brodribb et al. 2009). This is somewhat surprising, as minor veins (tertiary and above) make up most of the vascular volume in the leaf (Brodribb et al. 2007, Blonder et al. 2011, Sack et al. 2012, Price and Weitz 2014). For these 6 *Populus* genotypes, minor vein density (VLA_{minor}) accounts for ~99% of overall vein density – between 8 to 12 millimeters of minor veins in one square millimeter of leaf (Table 3.2).

Developmental characteristics likely account for this negative finding. Minor veins form with the expanding leaf, meaning minor veins can produce varying vein densities independent of final leaf size (Sack et al. 2012). While contrary to my initial hypothesis, this finding is upheld by previous studies across several species (Price and Weitz 2014, Carins-Murphy 2014, Flexas et al 2013, Xiong et al. 2014, Caringella et al. 2015, Sack et al. 2015). Other aspects unaccounted for by leaf anatomy may be driving differences in minor vein density in *Populus* genotypes.

4.3 Petiole xylem area and conductivity

4.3.1 Xylem area in the petiole

While leaf lamina parameters did not correlate with K_{leaf} or g_s, petiole hydraulic traits emerged as an important indicator of stomatal performance among *Populus* genotypes. Leaves are

commonly described as a hydraulic bottleneck of whole-plant performance (Sack et al. 2004, Sack and Holbrook 2006), yet the leaf petiole physically acts as a bottleneck to leaf water supply. Therefore, the petiole could potentially limit the entire downstream leaf performance by hydraulic architecture alone.

Fundamental work in hydraulic architecture in stems has examined the tradeoff between vessel size and cavitation (Tyree and Sperry 1989, Hacke and Sperry 2001, Wheeler et al. 2005, Tyree and Zimmerman 2002). These ideas may hold true in leaves as well, as larger vessels in the midrib may create an inherently more vulnerable xylem (Sack et al. 2015). After measuring vessel diameter (D_v), petiole area (A_p), and total xylem area in the petiole (A_x), it was clear that petiole xylem area seems to directly support leaf stomatal conductance and lamina area (Fig. 3.7).

This relationship likely represents the theory of allometric scaling, which essentially explains how features change with size in all living organisms (West et al. 2000, West and Brown 2005). Simply put, allometric scaling laws indicate that the dimensions of an organism will retain the same ratio regardless of size. For example, a large elephant would have thicker bones than a small cat, yet both would have the same ratio of bone density to body size.

For petioles and leaves, the same allometric rules apply. A larger xylem area would support greater water supply, allowing a larger leaf lamina to be created and sustained. Additionally, higher water flow would keep the mesophyll hydrated, a requirement for continuous stomatal conductance (Sack and Holbrook 2006, Sack et al. 2012). Interestingly, xylem area in the petiole was unrelated to the size of the vessel elements themselves (Table 3.2). This implies that total

xylem area retains the same ratio to petiole area, regardless of environmental conditions. Therefore, whether a plant will have large or small vessels will be independent of xylem area.

This match of hydraulic supply and demand in petioles and leaves has also been seen in stem parameters, suggesting that xylem area influences leaf area (Sack and Holbrook 2006, Plavcová et al. 2011). Plavcová and Hacke (2012) found that leaf area scaled linearly with native stem conductivity across drought, fertilization, and shade treatments in hybrid poplars. Similar to my findings above, this suggests that leaf area is controlled by the hydraulic transport capacity of the xylem (Plavcová and Hacke 2012, Hacke 2015), and that allometric scaling is involved in these functional traits.

4.3.2 Theoretical petiole conductivity

K_{leaf} measurements were unable to quantify conductance values for the *Populus* sp, but luckily another tool exists to quantify water flow: theoretical petiole conductivity. Previous researchers have used petiole conductivity as a physiological parameter – both measured and calculated (Schultz and Matthews 1993, Tyree and Ewers 1991, Zwieniecki et al. 2000). As petiole xylem area proved to be a strong determinant of leaf area and stomatal conductance, it seemed pertinent to calculate theoretical petiole conductivity (section 2.4.4 in methods).

In Figure 3.5, we see a strong positive relationship between theoretical petiole conductivity ($K_{h.petiole}$) and stomatal conductance (g_s). This trend is evident when including aspen (dashed line, r^2=0.85), but is even stronger without it (r^2 = 0.99). Similar to xylem area in the petiole, this finding implies that a higher rate of petiole conductivity directly supports stomatal conductance.

Petiole conductivity also positively correlated with leaf area, perhaps demonstrating that higher stomatal conductance would support higher carbon uptake and biomass production.

It is important to note, however, that this calculated conductivity is based upon perfect cylindrical pipes – meaning calculated conductivity will always be an overestimate (likely two-fold; Sperry and Pockman 1993, Sperry et al. 2003, McCulloh and Sperry 2005). Despite this fact, petiole conductivity is clearly linked with performance (g_s). Therefore, I suggest that in experiments where K_{leaf} is unable to explain hydraulic variation in leaves, petiole conductivity (either measured or calculated) might elucidate important patterns.

4.3.3 Leaf hydraulic conductance: why no correlations?

As previously discussed, leaf anatomical traits were unable to explain variations in K_{leaf} values among hybrid poplar clones (see Table A3; Fig. A4). In answer to my first experimental question, I did find variation across genotypes in leaf hydraulic performance, but was unable to explain these variations through leaf anatomy.

There are a few reasons that could account for this finding. Firstly, there have been several previous reports of K_{leaf} not correlating with leaf anatomical parameters as predicted (Flexas et al. 2013, Xiong et al. 2015, Caringella et al. 2015), indicating that K_{leaf} might not reflect hydraulic differences, especially at a genus level. It is also possible that our method for measuring K_{leaf} did not capture the complex nature of these hybrid poplars. Most reports indicate that leaves on the EFM apparatus will reach steady flow after 30 minutes (Sack and Scoffoni 2012, Laur and Hacke 2014b), but some of the poplar leaves in my study needed almost an hour

to reach a steady state. Stomatal activity could also be influencing the rate of flow, possibly undetected on the EFM. I think this method could be improved by measuring stomatal conductance of the leaf on the EFM, and by taking stomatal prints directly after disconnecting to measure the stomatal aperture.

Additionally, the petiole could drastically be influencing K_{leaf} by adding varying amounts of resistance. To my knowledge, there is no mention of the petiole influencing leaf hydraulic conductance in the EFM literature, which is surprising in context of my findings. Length of the petiole was not controlled for while attaching it to the tubing, and often differing amounts were removed per leaf. Additionally, no correction was made for petiole length. I suggest that future research in leaf hydraulics should separate K_{leaf} into both lamina and petiole conductance.

Other methods of measuring K_{leaf} (i.e. high pressure flow meter, rehydration kinetics) have drawbacks as well (Sack et al. 2002), emphasizing even more that leaves are complex systems (Sack and Holbrook 2006). This suggests to me that anatomy alone cannot explain K_{leaf}; or at least not within a genus. Ultimately, I conclude that alternate areas of resistance – like the extra-xylem pathway and membranes of living cells – are key factors influencing overall leaf hydraulics.

4.4 Extra-xylem pathways in the lamina

4.4.1 Characteristics of the bundle sheath and bundle sheath extensions

So far, this study has focused on the resistance of vein traits within the xylem. In Figures 3.7 and 3.8, we inspect hybrid poplar leaves from a cross-sectional perspective to understand the extra-

xylem pathway. As K_{leaf} encompasses water movement inside and outside the xylem (Sack and Holbrook 2006, Sack et al. 2012), it is possible that the anatomy of the bundle sheath and bundle sheath extensions exert greater resistance to water movement than previously believed.

Figure 3.8 (a-b) illustrates the extra-xylem vein anatomy found in poplar leaves. The bundle sheath (BS) encircles leaf minor veins with a layer of parenchyma cells, separating the vascular bundle from the comparatively dry air of the mesophyll (Heinen et al. 2009, Sack et al. 2015). The bundle sheath extensions (BSEs) extend vertically in two directions from minor veins, separating the palisade parenchyma (PP) and spongy mesophyll (SP) to connect with the epidermis (Figure 3.8a).

In Fig. 3.7, we see a strong positive correlation between minor vein area ($A_{minor.vein}$) and BSE area across (a) and within (b) *Populus* genotypes. Following the trend in previous figures, the poplar clones Green Giant, Okanese, and Northwest seem to have the largest $A_{minor.vein}$ and corresponding BSEs. P38 and Brooks have respectively small minor veins and BSEs, and aspen has the smallest mean values (Fig. 3.7a).

What is the importance of this positive correlation between $A_{minor.vein}$ and BSEs? How might these structures influence leaf hydraulic anatomy? Although both structures are critical to extra-xylem water flow, the BS (captured here in $A_{minor.vein}$) and BSEs have very different functions. The BS acts much like an endodermis in roots, preventing apoplastic flow and regulating water movement from the xylem through cell membranes (Heinen et al. 2009). The BS is believed to be a bottleneck to extra-xylem water flow (Shatil-Cohen et al. 2011, Sade et al. 2015) which is largely due to aquaporin regulation through the bundle sheath membrane (Heinen et al. 2009,

Shatil-Cohen et al. 2011, Sade et al. 2015, Sack et al. 2015). It is likely that AQPs are regulating hydraulic flow in the 6 *Populus* genotypes, but our study was unable to capture this activity.

In contrast, the bundle sheath extensions are believed to facilitate water flow to the epidermis (Wylie 1952, Buckley et al. 2011). Therefore, the pattern we see between $A_{\text{minor.vein}}$ and BSEs could be a relationship between "source" and "supply" of water in the leaf (Fig. 3.7). Alternative functions of the BSE may exist, so it is important to also examine the BSE anatomy (Fig. 4.5b). Firstly, BSE cells are shown to be are densely packed with small intercellular spaces. These cells lack chloroplasts (or at least have fewer than adjacent mesophyll cells), suggesting BSE cells contribute little to gas exchange and photosynthesis. BSE cells are also unlikely to exert rigid physical support, as the thin, unstained cell walls appear too weak to mechanically support the lamina. This is especially evident when compared to the highly lignified support fibers surrounding the vascular bundle (4.5d).

However, the anatomy of BSE cells could allow them to function instead as turgor-driven support. Such a turgor-driven system would have many advantages to the lamina, like increased flexibility. For example, turgor-enlarged BSE cells would allow full extension of the lamina under full hydration, and partial folding of the lamina when water supply decreases. This idea is similar to bulliform cells in *Poaceace* leaves, which function similarly and are vital in reducing water loss from the leaf.

Perhaps most important, however, is the proposed role BSEs play in water movement. Recent research has hypothesized that the main function is water transport from the BS to the epidermis (Buckley et al. 2011, Sack et al. 2015). In tomato, Zsögön et al. (2015) found that mutant tomato (*Solanum lycopersicum*) leaves that lacked BSEs had lower K_{leaf} and g_s than wild-type leaves,

implying that leaves without BSEs had a reduced ability to distribute water. Buckley et al. (2011) also found that BSEs increased hydraulic contact between the BS and epidermis, suggesting that BSEs are an important component to the leaf hydraulic pathway. This theory is supported by Figure 3.7, as larger veins have larger BSEs and could support the linear increase in water delivered to the epidermis. Our finding indirectly supports the theory that BSEs are an important component of the leaf hydraulic pathway.

4.5 Conclusions and future directions

Our findings support the idea that leaf anatomy influences hydraulic performance in hybrid poplar clones and trembling aspen. Leaf area, major vein density, total xylem area in the petiole, and theoretical petiole conductivity emerged as the strongest parameters of physiology and performance, especially in relation to stomatal conductance. While we were able to characterize variation in hydraulic traits across 6 *Populus* genotypes, we were unable to explain differences in leaf hydraulic conductance with leaf anatomy as hypothesized. Petiole hydraulic properties emerged as the strongest anatomical proxies of high performance, and thus should be considered when evaluating high-performance hybrid poplar clones.

This study raised many questions that would benefit from additional research. In particular, the extra-xylem pathway should be studied both through anatomy, fluorescent imaging, and other methods which would hopefully capture hydraulic regulation by aquaporins in the bundle sheath. It would be useful to study the above topics under ideal and drought conditions, to account for the additional role of aquaporins in refilling.

To explore the variation and consistency hybrid poplars exhibited in leaf area, a future study should investigate the phenotypic plasticity of hybrid poplar clones in the field. Currently, there is an experimental plantation established at the Devonian Botanical Garden in Edmonton, AB, containing all 5 of the hybrid poplar clones. Leaf anatomy and hydraulic performance could be measured during the next growing season and compared to the results from our greenhouse study. Through continued effort and ingenuity, we may yet explain how leaf anatomy shapes and is shaped by hydraulic demand.

References

Aasamaa, K., A. Sõber, and M. Rahi. 2001. Leaf anatomical characteristics associated with shoot hydraulic conductance, stomatal conductance and stomatal sensitivity to changes of leaf water status in temperate deciduous trees. Functional Plant Biology **28**:765-774.

Ache, P., H. Bauer, H. Kollist, K. A. Al-Rasheid, S. Lautner, W. Hartung, and R. Hedrich. 2010. Stomatal action directly feeds back on leaf turgor: new insights into the regulation of the plant water status from non-invasive pressure probe measurements. The Plant Journal **62**:1072-1082.

Allen, C. D., A. K. Macalady, H. Chenchouni, D. Bachelet, N. McDowell, M. Vennetier, T. Kitzberger, A. Rigling, D. D. Breshears, E. H. Hogg, P. Gonzalez, R. Fensham, Z. Zhang, J. Castro, N. Demidova, J.-H. Lim, G. Allard, S. W. Running, A. Semerci, and N. Cobb. 2010. A global overview of drought and heat-induced tree mortality reveals emerging climate change risks for forests. Forest Ecology and Management **259**:660-684.

Almeida-Rodriguez, A. M. and U. G. Hacke. 2012. Cellular localization of aquaporin mRNA in hybrid poplar stems. American Journal of Botany **99**:1249-1254.

Almeida-Rodriguez, A. M., U. G. Hacke, and J. Laur. 2011. Influence of evaporative demand on aquaporin expression and root hydraulics of hybrid poplar. Plant, Cell & Environment **34**:1318-1331.

Almeida-Rodriguez, A. M., J. E. Cooke, F. Yeh, and J. J. Zwiazek. 2010. Functional characterization of drought-responsive aquaporins in *Populus balsamifera* and *Populus simonii*× *balsamifera* clones with different drought resistance strategies. Physiologia Plantarum **140**:321-333.

Arango-Velez, A., J. J. Zwiazek, B. R. Thomas, and M. T. Tyree. 2011. Stomatal factors and vulnerability of stem xylem to cavitation in poplars. Physiologia Plantarum **143**:154-165.

Barigah, T., B. Saugier, M. Mousseau, J. Guittet, and R. Ceulemans. 1994. Photosynthesis, leaf area and productivity of 5 poplar clones during their establishment year. Annales des Sciences Forestières:613-625.

Beerling, D. J. 2005. Leaf evolution: gases, genes and geochemistry. Annals of Botany **96**:345-352.

Beerling, D. J., C. P. Osborne, and W. G. Chaloner. 2001. Evolution of leaf-form in land plants linked to atmospheric CO_2 decline in the Late Palaeozoic era. Nature **410**:352-354.

Blonder, B., C. Violle, L. P. Bentley, and B. J. Enquist. 2011. Venation networks and the origin of the leaf economics spectrum. Ecology Letters **14**:91-100.

Blonder, B., C. Violle, and B. J. Enquist. 2013. Assessing the causes and scales of the leaf economics spectrum using venation networks in *Populus tremuloides*. Journal of Ecology **101**:981-989.

Boyce, C. K. 2008. The fossil record of plant physiology and development: what leaves can tell us. Paleontology Society Papers **14**:133-146.

Boyce, C. K., T. J. Brodribb, T. S. Feild, and M. A. Zwieniecki. 2009. Angiosperm leaf vein evolution was physiologically and environmentally transformative. Proceedings of the Royal Society Biological Sciences:1919.

Boyer, J. 1977. Regulation of water movement in whole plants. Symposia of the Society for Experimental Biology:455.

Bradshaw, H., R. Ceulemans, J. Davis, and R. Stettler. 2000. Emerging model systems in plant biology: poplar (*Populus*) as a model forest tree. Journal of Plant Growth Regulation **19**:306-313.

Brodribb, T. J. 2009. Xylem hydraulic physiology: the functional backbone of terrestrial plant productivity. Plant Science **177**:245-251.

Brodribb, T. J. and T. S. Feild. 2010. Leaf hydraulic evolution led a surge in leaf photosynthetic capacity during early angiosperm diversification. Ecology Letters **13**:175-183.

Brodribb, T. J., T. S. Feild, and G. J. Jordan. 2007. Leaf maximum photosynthetic rate and venation are linked by hydraulics. Plant Physiology **144**:1890-1898.

Brodribb, T. J. and N. M. Holbrook. 2003. Changes in leaf hydraulic conductance during leaf shedding in seasonally dry tropical forest. New Phytologist **158**:295-303.

Brown, J. H. and G. B. West. 2000. Scaling in biology. Oxford University Press.

Buckley, T. N. 2015. The contributions of apoplastic, symplastic and gas phase pathways for water transport outside the bundle sheath in leaves. Plant, Cell & Environment **38**:7-22.

Buckley, T. N., L. Sack, and M. E. Gilbert. 2011. The role of bundle sheath extensions and life form in stomatal responses to leaf water status. Plant Physiology **156**:962-973.

Caringella, M. A., F. J. Bongers, and L. Sack. 2015 (in press). Leaf hydraulic conductance varies with vein anatomy across *Arabidopsis thaliana* wild-type and leaf vein mutants. Plant, Cell & Environment. doi: 10.1111/pce.12584.

Carins Murphy, M. R., G. J. Jordan, and T. J. Brodribb. 2014. Acclimation to humidity modifies the link between leaf size and the density of veins and stomata. Plant, Cell & Environment **37**:124-131.

Ceulemans, R., R. F. Stettler, T. M. Hinckley, J. G. Isebrands, and P. E. Heilman. 1990. Crown architecture of *Populus* clones as determined by branch orientation and branch characteristics. Tree physiology **7**:157-167.

Ellis, B., D. C. Daly, L. J. Hickey, K. R. Johnson, J. D. Mitchell, P. Wilf, and S. L. Wing. 2009. Manual of leaf architecture. Cornell University Press Ithaca.

Flexas, J., C. Scoffoni, J. Gago, and L. Sack. 2013. Leaf mesophyll conductance and leaf hydraulic conductance: an introduction to their measurement and coordination. Journal of Experimental Botany **64**:3965-3981.

Gupta, A. B. and R. Sankararamakrishnan. 2009. Genome-wide analysis of major intrinsic proteins in the tree plant *Populus trichocarpa*: characterization of XIP subfamily of aquaporins from evolutionary perspective. BMC Plant Biology **9**:134.

Hacke, U. and J. J. Sauter. 1996. Drought-induced xylem dysfunction in petioles, branches, and roots of *Populus balsamifera* L. and *Alnus glutinosa* (L.) Gaertn. Plant Physiology **111**:413-417.

Hacke, U. G. 2015. The Hydraulic Architecture of *Populus*. Pages 103-131 Functional and Ecological Xylem Anatomy. Springer.

Hacke, U. G. and J. S. Sperry. 2001. Functional and ecological xylem anatomy. Perspectives in Plant Ecology, Evolution and Systematics **4**:97-115.

Hacke, U. G., J. S. Sperry, J. K. Wheeler, and L. Castro. 2006. Scaling of angiosperm xylem structure with safety and efficiency. Tree Physiology **26**:689-701.

Heinen, R. B., Q. Ye, and F. Chaumont. 2009. Role of aquaporins in leaf physiology. Journal of experimental botany **60**:2971-2985.

Kramer, P. J. and J. S. Boyer. 1995. Water relations of plants and soils. Academic press.

Larson, P. R. and J. Isebrands. 1971. The plastochron index as applied to developmental studies of cottonwood. Canadian Journal of Forest Research **1**:1-11.

Laur, J. and U. G. Hacke. 2014a. Exploring *Picea glauca* aquaporins in the context of needle water uptake and xylem refilling. New Phytologist **203**:388-400.

Laur, J. and U. G. Hacke. 2014b. The Role of Water Channel Proteins in Facilitating Recovery of Leaf Hydraulic Conductance from Water Stress in *Populus trichocarpa*. PloS one **9**:e111751.

Lucas, W. J., A. Groover, R. Lichtenberger, K. Furuta, S. R. Yadav, Y. Helariutta, X. Q. He, H. Fukuda, J. Kang, and S. M. Brady. 2013. The plant vascular system: evolution, development and functions. Journal of Integrative Plant Biology **55**:294-388.

Martre, P., R. Morillon, F. Barrieu, G. B. North, P. S. Nobel, and M. J. Chrispeels. 2002. Plasma membrane aquaporins play a significant role during recovery from water deficit. Plant Physiology **130**:2101-2110.

McCulloh, K. A. and J. S. Sperry. 2005. Patterns in hydraulic architecture and their implications for transport efficiency. Tree Physiology **25**:257-267.

Michaelian, M., E. H. Hogg, R. J. Hall, and E. Arsenault. 2011. Massive mortality of aspen following severe drought along the southern edge of the Canadian boreal forest. Global Change Biology **17**:2084-2094.

Nardini, A., E. Õunapuu-Pikas, and T. Savi. 2014. When smaller is better: leaf hydraulic conductance and drought vulnerability correlate to leaf size and venation density across four *Coffea arabica* genotypes. Functional Plant Biology **41**:972-982.

Orlovic, S., V. Guzina, B. Krstic, and L. Merkulov. 1998. Genetic variability in anatomical, physiological and growth characteristics of hybrid poplar (*Populus* x *euramericana* Dode

(Guinier)) and eastern cottonwood (*Populus deltoides* Bartr.) clones. Silvae Genetica **47**:183-189.

Pallardy, S. G. 2010. Physiology of Woody Plants. Academic Press.

Pittermann, J. and J. Sperry. 2003. Tracheid diameter is the key trait determining the extent of freezing-induced embolism in conifers. Tree Physiology **23**:907-914.

Plavcová, L. and U. G. Hacke. 2012. Phenotypic and developmental plasticity of xylem in hybrid poplar saplings subjected to experimental drought, nitrogen fertilization, and shading. Journal of Experimental Botany 63: 6481-6491.

Plavcova, L., U. G. Hacke, and J. S. Sperry. 2011. Linking irradiance-induced changes in pit membrane ultrastructure with xylem vulnerability to cavitation. Plant, Cell & Environment **34**:501-513.

Price, C. A. and J. S. Weitz. 2014. Costs and benefits of reticulate leaf venation. BMC Plant Biology **14**:234.

R Core Team (2013). R: A language and environment for statistical computing. R Foundation for Statistical Computing, Vienna, Austria. SBN 3-900051-07-0, URL http://www.R-project.org/.

Ridge, C. R., T. M. Hinckley, R. F. Stettler, and E. Van Volkenburgh. 1986. Leaf growth characteristics of fast-growing poplar hybrids *Populus trichocarpa* × *P. deltoides*. Tree physiology **1**:209-216.

Sack, L., P. Cowan, N. Jaikumar, and N. Holbrook. 2003. The 'hydrology'of leaves: co-ordination of structure and function in temperate woody species. Plant, Cell & Environment **26**:1343-1356.

Sack, L., E. M. Dietrich, C. M. Streeter, D. Sánchez-Gómez, and N. M. Holbrook. 2008. Leaf palmate venation and vascular redundancy confer tolerance of hydraulic disruption. Proceedings of the National Academy of Sciences **105**:1567-1572.

Sack, L. and K. Frole. 2006. Leaf structural diversity is related to hydraulic capacity in tropical rain forest trees. Ecology **87**:483-491.

Sack, L. and N. M. Holbrook. 2006. Leaf hydraulics. Annual Review of Plant Biology. **57**:361-381.

Sack, L., P. J. Melcher, M. A. Zwieniecki, and N. M. Holbrook. 2002. The hydraulic conductance of the angiosperm leaf lamina: a comparison of three measurement methods. Journal of Experimental Botany **53**:2177-2184.

Sack, L. and C. Scoffoni. 2012. Measurement of leaf hydraulic conductance and stomatal conductance and their responses to irradiance and dehydration using the Evaporative Flux Method (EFM). Journal of visualized experiments: JoVE.

Sack, L. and C. Scoffoni. 2013. Leaf venation: structure, function, development, evolution, ecology and applications in the past, present and future. New Phytologist **198**:983-1000.

Sack, L., C. Scoffoni, G. P. John, H. Poorter, C. M. Mason, R. Mendez-Alonzo, and L. A. Donovan. 2013. How do leaf veins influence the worldwide leaf economic spectrum? Review and synthesis. Journal of experimental botany **64**:4053-4080.

Sack, L., C. Scoffoni, D. M. Johnson, T. N. Buckley, and T. J. Brodribb. 2015. The Anatomical Determinants of Leaf Hydraulic Function. Pages 255-271 Functional and Ecological Xylem Anatomy. Springer.

Sack, L., C. Scoffoni, A. D. McKown, K. Frole, M. Rawls, J. C. Havran, H. Tran, and T. Tran. 2012. Developmentally based scaling of leaf venation architecture explains global ecological patterns. Nature Communications **3**:837.

Sack, L., C. M. Streeter, and N. M. Holbrook. 2004. Hydraulic analysis of water flow through leaves of sugar maple and red oak. Plant Physiology **134**:1824-1833.

Sack, L., M. T. Tyree, and N. M. Holbrook. 2005. Leaf hydraulic architecture correlates with regeneration irradiance in tropical rainforest trees. New Phytologist **167**:403-413.

Sade, N., A. Shatil-Cohen, Z. Attia, C. Maurel, Y. Boursiac, G. Kelly, D. Granot, A. Yaaran, S. Lerner, and M. Moshelion. 2014. The role of plasma membrane aquaporins in regulating the bundle sheath-mesophyll continuum and leaf hydraulics. Plant Physiology **166**:1609-1620.

Sade, N., A. Shatil-Cohen, and M. Moshelion. 2015. Bundle-sheath aquaporins play a role in controlling *Arabidopsis* leaf hydraulic conductivity. Plant signaling & behavior **10**:e1017177.

Scarpella, E., M. Barkoulas, and M. Tsiantis. 2010. Control of leaf and vein development by auxin. Cold Spring Harbor Perspectives in Biology **2**:a001511.

Scarpella, E., P. Francis, and T. Berleth. 2004. Stage-specific markers define early steps of procambium development in *Arabidopsis* leaves and correlate termination of vein formation with mesophyll differentiation. Development **131**:3445-3455.

Scarpella, E., D. Marcos, J. Friml, and T. Berleth. 2006. Control of leaf vascular patterning by polar auxin transport. Genes & Development **20**:1015-1027.

Schreiber, S. G., C. Ding, A. Hamann, U. G. Hacke, B. R. Thomas, and J. S. Brouard. 2013a. Frost hardiness vs. growth performance in trembling aspen: an experimental test of assisted migration. Journal of Applied Ecology **50**:939-949.

Schreiber, S. G., U. G. Hacke, S. Chamberland, C. W. Lowe, D. Kamelchuk, K. Bräutigam, M. M. Campbell, and B. R. Thomas. 2015 (in press). Leaf size serves as a proxy for xylem vulnerability to cavitation in plantation trees. Plant, Cell & Environment.

Schreiber, S. G., U. G. Hacke, A. Hamann, and B. R. Thomas. 2011. Genetic variation of hydraulic and wood anatomical traits in hybrid poplar and trembling aspen. New Phytologist **190**:150-160.

Schreiber, S. G., A. Hamann, U. G. Hacke, and B. R. Thomas. 2013b. Sixteen years of winter stress: an assessment of cold hardiness, growth performance and survival of hybrid poplar clones at a boreal planting site. Plant, Cell & Environment **36**:419-428.

Schultz, H. R. and M. A. Matthews. 1993. Xylem development and hydraulic conductance in sun and shade shoots of grapevine (*Vitis vinifera* L.): evidence that low light uncouples water transport capacity from leaf area. Planta **190**:393-406.

Scoffoni, C. 2015. Modelling the outside-xylem hydraulic conductance: towards a new understanding of leaf water relations. Plant, Cell & Environment **38**:4-6.

Scoffoni, C., M. Rawls, A. McKown, H. Cochard, and L. Sack. 2011. Decline of leaf hydraulic conductance with dehydration: relationship to leaf size and venation architecture. Plant Physiology **156**:832-843.

Scoffoni, C. a. L. S. 2013. Quantifying leaf vein traits. PrometheusWiki. CSIRO.

Settler, R. F. and C. National Research Council. 1998. Biology of *Populus* and Its Implications for Management and Conservation. NRC Research Press, Ottawa.

Shatil-Cohen, A. and M. Moshelion. 2012. Smart pipes: the bundle sheath role as xylem-mesophyll barrier. Plant Signaling & Behavior **7**:1088-1091.

Shatil-Cohen, A., Z. Attia, and M. Moshelion. 2011. Bundle-sheath cell regulation of xylem-mesophyll water transport via aquaporins under drought stress: a target of xylem-borne ABA? The Plant Journal **67**:72-80.

Sperry, J. and W. Pockman. 1993. Limitation of transpiration by hydraulic conductance and xylem cavitation in *Betula occidentalis*. Plant, Cell & Environment **16**:279-287.

Sperry, J. S. 2003. Evolution of water transport and xylem structure. International Journal of Plant Sciences **164**:S115-S127.

Sperry, J. S. and U. G. Hacke. 2004. Analysis of circular bordered pit function I. Angiosperm vessels with homogenous pit membranes. American Journal of Botany **91**:369-385.

Sperry, J. S., U. G. Hacke, and J. Pittermann. 2006. Size and function in conifer tracheids and angiosperm vessels. American Journal of Botany **93**:1490-1500.

Taylor, G. 2002. *Populus*: *Arabidopsis* for forestry. Do we need a model tree? Annals of Botany **90**:681-689.

Tuskan, G. A., S. Difazio, S. Jansson, J. Bohlmann, I. Grigoriev, U. Hellsten, N. Putnam, S. Ralph, S. Rombauts, and A. Salamov. 2006. The genome of black cottonwood, *Populus trichocarpa* (Torr. & Gray). Science **313**:1596-1604.

Tyree, M. and M. Zimmermann. 2002. Xylem Structure and the Ascent of Sap, Springer. Berlin, Germany.

Tyree, M. T. and F. W. Ewers. 1991. The hydraulic architecture of trees and other woody plants. New Phytologist **119**:345-360.

Tyree, M. T. and J. S. Sperry. 1989. Vulnerability of xylem to cavitation and embolism. Annual review of plant biology **40**:19-36.

Voicu, M. and J. Zwiazek. 2011. Diurnal and seasonal changes of leaf lamina hydraulic conductance in bur oak (*Quercus macrocarpa*) and trembling aspen (*Populus tremuloides*). Trees **25**:485-495.

Voicu, M. C., J. J. Zwiazek, and M. T. Tyree. 2008. Light response of hydraulic conductance in bur oak (*Quercus macrocarpa*) leaves. Tree physiology **28**:1007-1015.

West, G. B. and J. H. Brown. 2005. The origin of allometric scaling laws in biology from genomes to ecosystems: towards a quantitative unifying theory of biological structure and organization. Journal of Experimental Biology **208**:1575-1592.

Wheeler, J. K., J. S. Sperry, U. G. Hacke, and N. Hoang. 2005. Inter-vessel pitting and cavitation in woody Rosaceae and other vesselled plants: a basis for a safety versus efficiency trade-off in xylem transport. Plant, Cell & Environment **28**:800-812.

Wylie, R. B. 1952. The bundle sheath extension in leaves of dicotyledons. American Journal of Botany:645-651.

Xiong, D., T. Yu, T. Zhang, Y. Li, S. Peng, and J. Huang. 2014. Leaf hydraulic conductance is coordinated with leaf morpho-anatomical traits and nitrogen status in the genus Oryza. Journal of Experimental Botany 66: 741-748.

Zsögön, A., A. C. Alves Negrini, L. E. P. Peres, H. T. Nguyen, and M. C. Ball. 2015. A mutation that eliminates bundle sheath extensions reduces leaf hydraulic conductance, stomatal conductance and assimilation rates in tomato (*Solanum lycopersicum*). New Phytologist **205**:618-626.

Zwieniecki, M., P. Melcher, C. Boyce, L. Sack, and N. Holbrook. 2002. Hydraulic architecture of leaf venation in *Laurus nobilis* L. Plant, Cell & Environment **25**:1445-1450.

Zwieniecki, M. A., T. J. Brodribb, and N. M. Holbrook. 2007. Hydraulic design of leaves: insights from rehydration kinetics. Plant, Cell & Environment **30**:910-921.

Appendix

Table A1: A list of abbreviations, descriptions, and units of hydraulic parameters measured in aspen and hybrid poplar clones.

Abbreviation	Definition	Units
A_L	Total leaf area	mm^2
1° VLA	Primary (midvein) vein length per area (i.e. vein density)	$mm\ mm^{-2}$
2° VLA	Secondary vein length per area	$mm\ mm^{-2}$
3° VLA	Tertiary vein length per area	$mm\ mm^{-2}$
4+° VLA	Quaternary and higher vein length per area	$mm\ mm^{-2}$
VLA_{major} (1+2)	Major vein density (primary and secondary)	$mm\ mm^{-2}$
VLA_{minor} (3+)	Minor vein density (tertiary, quaternary, and higher)	$mm\ mm^{-2}$
LMA	Leaf mass per area	$g\ m^{-2}$
T_{leaf}	Leaf lamina thickness	mm
A_p	Area of the petiole	cm^2
A_x	Total xylem area in the petiole	cm^2
D_V	Mean vessel diameter, hydraulically weighted	µm
$K_{h.petiole}$	Theoretical petiole conductivity	$Kg\ m\ MPa^{-1}\ s^{-1}$
A_{BSE}	Bundle sheath extension (BSE) area of a minor vein (Fig. 3.8)	$µm^2$
$A_{minor\ vein}$	Minor vein area of corresponding BSE (Fig. 3.8)	$µm^2$
$D_{l.epidermis}$	Distance from xylem to lower epidermis, tracing cell walls	µm
$g_{s,\ total}$	Stomatal conductance of both abaxial (AB), adaxial (AD) surface	$mmol\ m^{-2}\ s^{-1}$
K_{Leaf}	Leaf hydraulic conductance	$mmol\ m^{-2}\ s^{-1}\ MPa^{-1}$
K_{Leaf}^{max}	Maximum leaf hydraulic conductance	$mmol\ m^{-2}\ s^{-1}\ MPa^{-1}$
Ht	Height of apical meristem	cm
T_{PP}	Thickness of the palisade parenchyma	µm
T_{SP}	Thickness of the spongy mesophyll	µm
T_{SP}: T_{PP}	Ratio of palisade to spongy mesophyll	µm

Table A2: Mean values of selected hydraulic traits for *Populus* genotypes. Standard error presented below mean value in parentheses. Please see Table A1 for the full name and units of each trait.

CLONE	A_L	VLA_{major}	VLA_{minor}	LMA	T_{leaf}	A_p	A_x	D_v	$K_{h.petiole}$	K_{Leaf}
Aspen	3167.94 (263.67)	0.09 (0.01)	9.31 (0.44)	398.78 (3.71)	0.15 (0.00)	1.18 (0.10)	0.08 (0.01)	13.20 (0.84)	3.402 E-07 (9.001 E-08)	7.63 (0.52)
Brooks	4361.86 (244.78)	0.11 (0.00)	10.57 (0.61)	589.98 (5.54)	0.22 (0.01)	1.70 (0.09)	0.14 (0.01)	16.40 (0.65)	1.011 E-06 (1.207 E-07)	4.44 (0.37)
Green Giant	4733.02 (356.08)	0.09 (0.00)	8.25 (0.30)	752.76 (3.86)	0.26 (0.01)	2.04 (0.17)	0.20 (0.02)	16.92 (0.59)	1.412 E-06 (1.551 E-07)	7.78 (1.07)
Northwest	6400.00 (238.24)	0.08 (0.00)	12.62 (0.28)	608.69 (2.34)	0.26 (0.01)	2.42 (0.08)	0.21 (0.00)	16.08 (0.54)	1.549 E-06 (2.112 E-07)	6.36 (0.41)
Okanese	4778.80 (258.91)	0.09 (0.00)	8.42 (0.36)	841.33 (2.51)	0.23 (0.01)	1.74 (0.08)	0.13 (0.01)	15.31 (0.45)	9.275 E-07 (1.006 E-07)	7.49 (0.53)
P38	3057.58 (184.18)	0.14 (0.01)	10.35 (0.39)	675.12 (1.50)	0.26 (0.00)	1.68 (0.07)	0.12 (0.01)	15.91 (0.97)	7.665 E-07 (8.473 E-08)	8.54 (0.58)

Table A2 cont'd: Means and standard errors of selected hydraulic traits, including both anatomy and physiology. Standard error presented below mean value in parentheses. Please see Table 3.1 for the full name and units of each trait.

CLONE	A_{BSE}	$A_{minor\ vein}$	$D_{L.epidermis}$	$g_{s,\ total}$	$g_{s,\ density}$ (AB)	$g_{s,\ density}$ (AD)	Ht	T_{PP}	T_{SP}	T_{SP}:T_{PP}
Aspen	2544.28 (165.79)	2958.13 (148.80)	89.27 (2.35)	273.17 (38.40)	123 (7.8)	0 (0.4)	33.5 (3.19)	72.04 (4.18)	55.36 (5.37)	0.77 (0.00)
Brooks	8722.17 (390.09)	4349.50 (328.20)	150.61 (3.91)	364.31 (33.72)	112 (4.1)	40 (2.9)	33.5 (1.79)	81.45 (3.27)	111.78 (6.16)	1.38 (0.00)
Green Giant	12682.13 (549.68)	4918.71 (383.43)	173.73 (4.97)	495.38 (43.84)	58 (2.4)	29 (2.0)	46.5 (1.87)	95.64 (3.06)	120.71 (9.31)	1.27 (0.00)
Northwest	10863.12 (668.29)	5684.54 (555.83)	183.34 (4.23)	538.13 (50.63)	108 (8.9)	58 (3.0)	46.4 (2.33)	80.45 (6.51)	132.55 (9.96)	1.66 (0.00)
Okanese	12010.22 (631.65)	5386.62 (384.17)	161.12 (2.91)	324.24 (60.55)	105 (5.0)	8 (2.1)	52.5 (3.33)	103.37 (3.64)	118.05 (12.96)	1.14 (0.00)
P38	8395.92 (460.96)	4416.37 (297.94)	187.02 (4.11)	252.13 (28.04)	153 (8.4)	65 (4.8)	56.7 (2.13)	81.03 (3.38)	157.09 (5.26)	1.95 (0.00)

Table 3.3: Correlation matrix of the means for hybrid poplar clones, with and without aspen. Values in the lower left represent mean values for aspen and all hybrid clones (Brooks, Green Giant, Northwest, Okanese, and P38P38), while those in the upper right, gray-shaded box contain just correlations between hybrid clones (no aspen). The Pearson's correlation coefficient is displayed on the top line, while the significance value for each interaction is displayed in parentheses below. Significant interactions ($P \leq 0.05$) are highlighted in bold, and values driven by aspen are shown in italics (see Fig. A3).

	A_L	1° VLA	2° VLA	3° VLA	4+° VLA	LMA	T_{leaf}	A_p
A_L		-0.91 **(0.033)**	-0.9 **(0.039)**	-0.62 (0.27)	0.39 (0.52)	-0.13 (0.83)	0.15 (0.81)	0.86 (0.06)
1° VLA	-0.91 **(0.012)**		0.87 (0.053)	0.74 (0.15)	-0.11 (0.87)	-0.18 (0.77)	-0.40 (0.50)	-0.87 (0.054)
2° VLA	-0.58 (0.23)	0.67 (0.14)		0.76 (0.13)	0.03 (0.97)	-0.16 (0.79)	0.08 (0.90)	-0.64 (0.24)
3° VLA	-0.38 (0.45)	0.58 (0.22)	0.78 (0.07)		0.2 (0.75)	-0.09 (0.89)	-0.26 (0.68)	-0.63 (0.26)
4+° VLA	0.42 (0.40)	-0.16 (0.76)	0.08 (0.87)	0.24 (0.65)		-0.84 (0.08)	0.21 (0.73)	0.51 (0.39)
LMA	0.32 (0.53)	-0.37 (0.48)	0.16 (0.76)	0.16 (0.76)	-0.36 (0.49)		-0.01 (0.99)	-0.26 (0.67)
T_{leaf}	0.5 (0.31)	-0.46 (0.36)	0.32 (0.54)	0.13 (0.80)	0.26 (0.62)	0.71 (0.12)		0.6 (0.28)
A_p	0.87 **(0.022)**	-0.8 (0.055)	-0.18 (0.73)	-0.22 (0.68)	0.47 (0.34)	0.47 (0.35)	*0.84* ***(0.038)***	
A_x	0.82 **(0.045)**	-0.81 **(0.049)**	-0.26 (0.61)	-0.45 (0.37)	0.31 (0.56)	0.43 (0.39)	0.79 (0.06)	0.95 **(0.003)**
D_V	0.47 (0.35)	-0.34 (0.51)	0.25 (0.63)	-0.02 (0.97)	0.16 (0.77)	0.63 (0.18)	*0.87* ***(0.024)***	0.75 (0.09)
$K_{h.petiole}$	0.86 **(0.027)**	-0.80 (0.057)	-0.25 (0.63)	-0.36 (0.48)	0.33 (0.52)	0.49 (0.32)	0.80 (0.056)	0.97 **(0.001)**
A_{BSE}	0.65 (0.16)	-0.64 (0.17)	-0.05 (0.93)	-0.1 (0.85)	-0.07 (0.89)	*0.89* ***(0.017)***	*0.85* ***(0.034)***	0.79 (0.06)
$A_{minor\ vein}$	0.81 **(0.049)**	-0.74 (0.09)	-0.12 (0.83)	0.02 (0.97)	0.24 (0.64)	0.76 (0.08)	*0.83* ***(0.041)***	0.89 **(0.019)**
$D_{l.epidermis}$	0.46 (0.35)	-0.38 (0.46)	0.40 (0.43)	0.28 (0.60)	0.30 (0.56)	0.71 (0.11)	0.99 **(0.00)**	0.80 (0.058)
$g_{s,\ total}$	0.88 **(0.021)**	-0.88 **(0.022)**	-0.54 (0.27)	-0.65 (0.16)	0.32 (0.54)	0.21 (0.69)	0.54 (0.27)	0.87 **(0.024)**
K_{Leaf}	-0.4 (0.43)	0.05 (0.93)	0.27 (0.61)	0.09 (0.87)	-0.42 (0.41)	0.21 (0.68)	0.1 (0.85)	-0.19 (0.72)

Table 3.3, cont'd: Correlation matrix of Pearson's correlation coefficients and significance values ($P \leq 0.05$ shown in bold). Hybrid poplar WITH aspen in lower left boxes, hybrid poplar WITHOUT aspen in upper right of table (shaded gray). Values in italics show correlations driven by aspen.

	A_x	D_V	$K_{h.petiole}$	A_{BSE}	$A_{minor\ vein}$	$D_{l.epidermis}$	$g_{s,\ total}$	K_{Leaf}
A_L	0.76 (0.14)	0.05 (0.94)	0.85 (0.07)	0.53 (0.36)	0.84 (0.07)	0.01 (0.98)	0.85 (0.07)	-0.36 (0.56)
1° VLA	-0.84 (0.08)	-0.1 (0.88)	-0.87 (0.054)	-0.79 (0.11)	-0.9 **(0.036)**	-0.2 (0.74)	-0.86 (0.06)	-0.02 (0.98)
2° VLA	-0.67 (0.22)	-0.11 (0.86)	-0.76 (0.14)	-0.75 (0.15)	-0.75 (0.14)	0.3 (0.63)	-0.79 (0.11)	0.36 (0.55)
3° VLA	-0.86 (0.06)	-0.68 (0.21)	-0.86 (0.06)	-0.74 (0.15)	-0.39 (0.52)	0.08 (0.90)	-0.88 (0.051)	0.15 (0.81)
4+° VLA	0.25 (0.69)	-0.04 (0.95)	0.29 (0.63)	-0.52 (0.37)	0.17 (0.79)	0.36 (0.55)	0.27 (0.66)	-0.4 (0.51)
LMA	-0.18 (0.77)	-0.38 (0.53)	-0.22 (0.73)	0.68 (0.21)	0.3 (0.63)	-0.08 (0.89)	-0.22 (0.73)	0.62 (0.27)
T_{leaf}	0.59 (0.30)	0.27 (0.66)	0.47 (0.43)	0.24 (0.70)	0.3 (0.62)	0.94 **(0.018)**	0.4 (0.51)	0.66 (0.23)
A_p	0.92 **(0.026)**	0.28 (0.65)	0.93 **(0.020)**	0.44 (0.46)	0.73 (0.16)	0.46 (0.44)	0.91 **(0.033)**	-0.06 (0.92)
A_x		0.58 (0.30)	0.99 **(0.002)**	0.56 (0.32)	0.56 (0.33)	0.34 (0.57)	0.97 **(0.005)**	-0.06 (0.93)
D_V	0.78 (0.07)		0.52 (0.37)	0.1 (0.88)	-0.33 (0.58)	0.02 (0.98)	0.54 (0.35)	-0.2 (0.74)
$K_{h.petiole}$	0.99 **(0.000)**	0.82 **(0.048)**		0.7 (0.19)	0.76 (0.14)	0.66 (0.23)	0.92 **(0.009)**	0.5 (0.40)
A_{BSE}	0.78 (0.07)	0.83 ***(0.042)***	0.83 ***(0.042)***		0.68 (0.21)	-0.02 (0.98)	0.57 (0.32)	0.29 (0.64)
$A_{minor\ vein}$	0.78 (0.07)	0.69 (0.13)	0.84 ***(0.035)***	0.91 **(0.011)**		0.23 (0.71)	0.59 (0.29)	0.12 (0.85)
$D_{l.epidermis}$	0.71 (0.12)	0.85 ***(0.033)***	0.74 (0.09)	*0.82* ***(0.048)***	*0.83* ***(0.043)***		0.15 (0.81)	0.68 (0.21)
$g_{s,\ total}$	0.94 **(0.005)**	0.58 (0.22)	1.0 **(0.001)**	0.61 (0.20)	0.65 (0.17)	0.44 (0.38)		-0.25 (0.68)
K_{Leaf}	-0.17 (0.74)	-0.26 (0.61)	-0.27 (0.60)	-0.04 (0.93)	-0.11 (0.84)	0.07 (0.90)	-0.31 (0.55)	

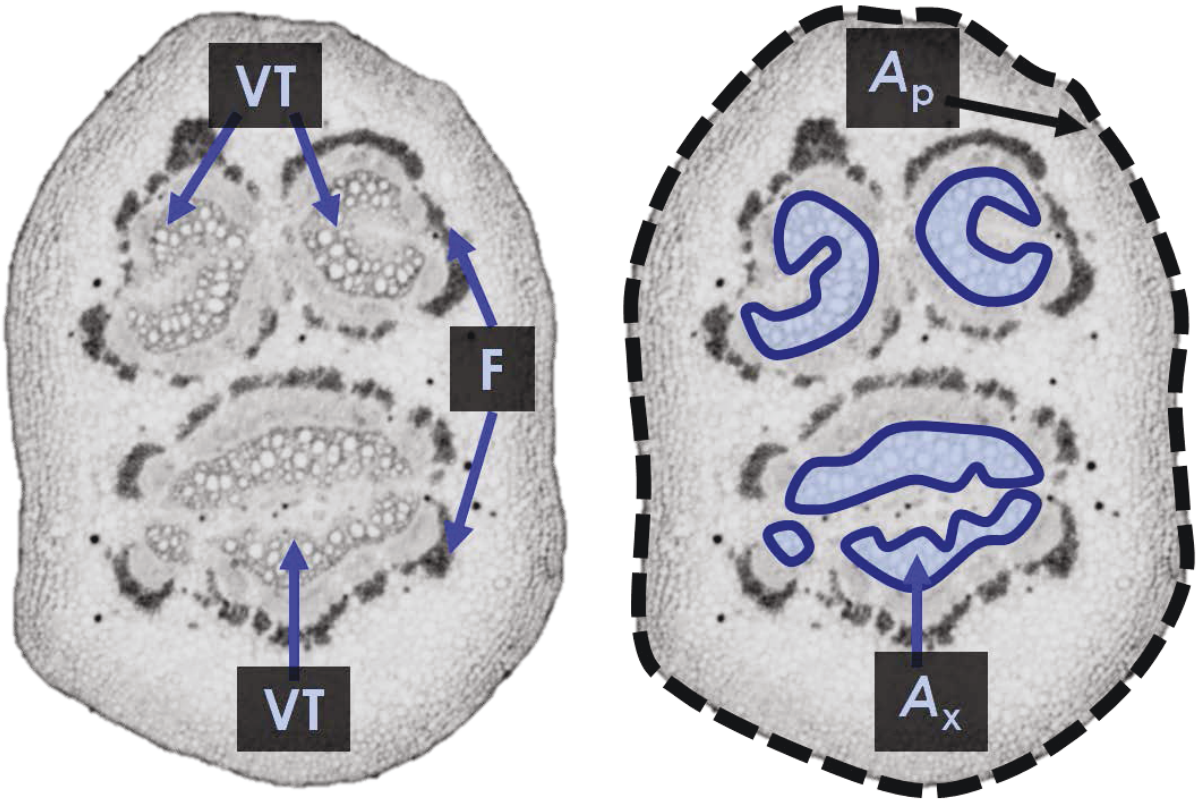

Figure A1: Petiole cross-sections showing vascular traces/bundles (VT), fibers (F), petiole area (A_p), and total xylem area (A_x).

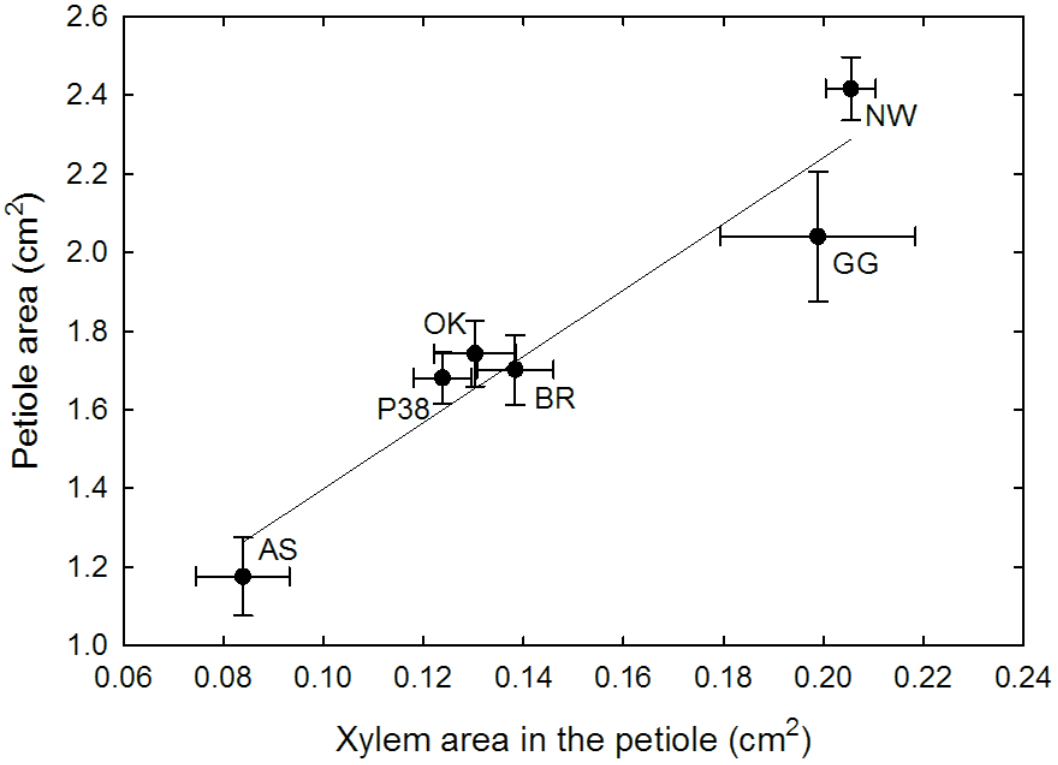

Figure A2: Xylem area in the petiole scales linearly with petiole area ($r^2 = 0.91$, $p < 0.01$).

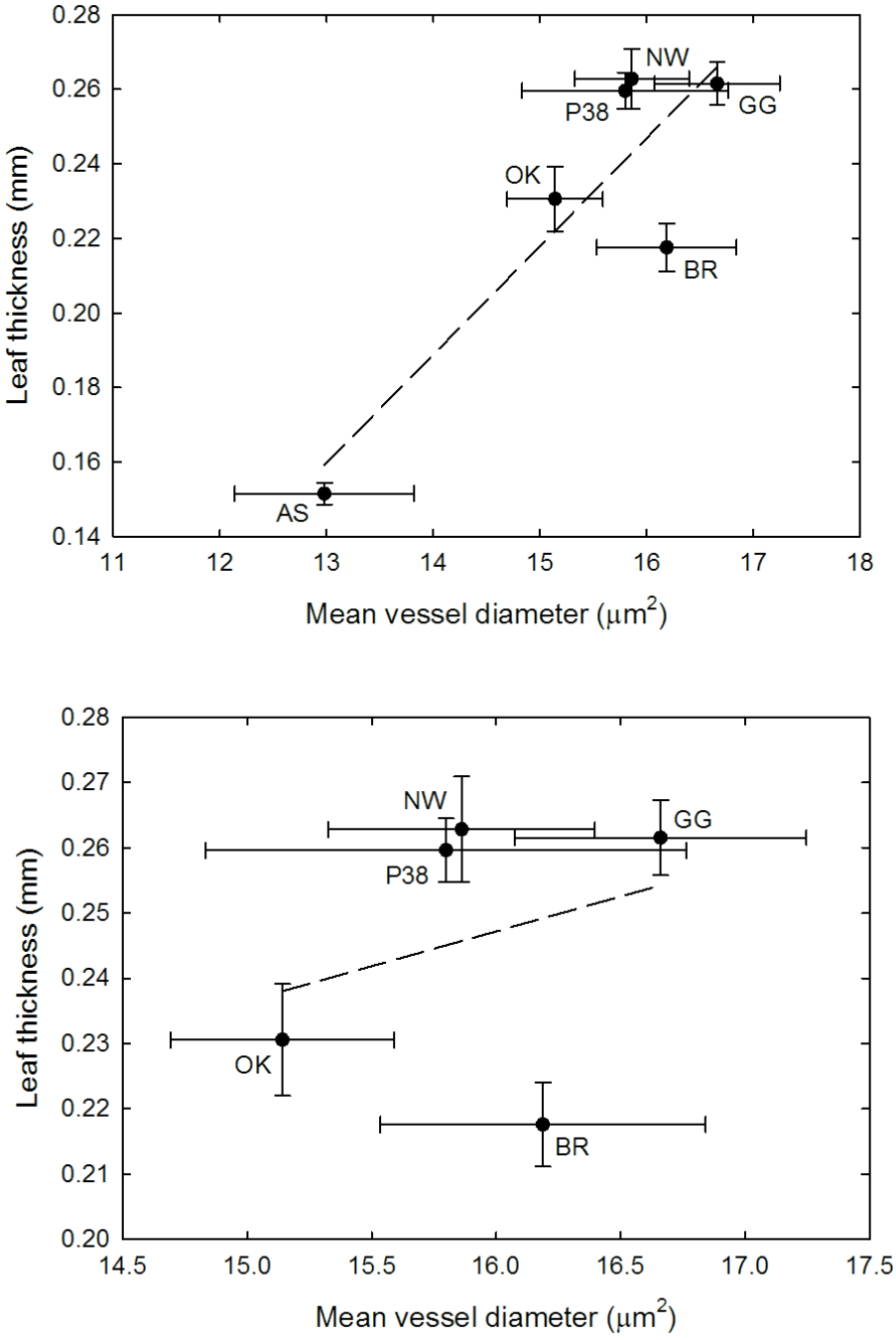

Figure A3: Two figures of leaf anatomy, selected to illustrate the italicized values in the tables above (Table 3.3). It is clear in (a) that aspen drives the linear regression ($r^2 = 0.77$, $P = 0.023$), as the trend is weak without aspen (b). When the data is separated into clone means, the trend is not significant ($P = 0.23$).

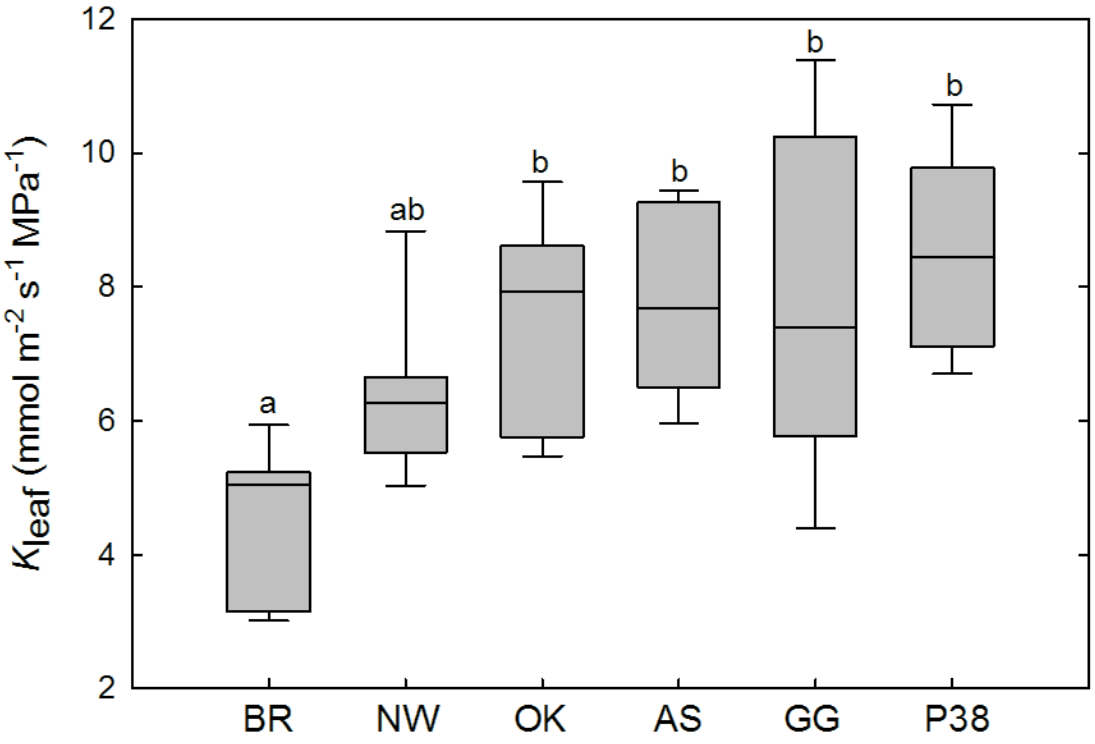

Figure A4: Leaf hydraulic conductance among *Populus* sp [Brooks (BR), Northwest (NW), Okanese (OK), Aspen (AS), Green Giant (GG), and P38P38 (P38)]. Median of the data is represented by the black line within the shaded box. Whiskers represent 10% (lower) and 90% (upper) percentiles. Box limits on either side of the median represent 25% (lower) and 75% (upper) percentiles. Letters indicate significant ($p \leq 0.01$) differences between hybrid poplars, as derived from a Tukey post-hoc test after a One-way ANOVA.